Controls on formation and alteration of early diagenetic dolomite: A multi-proxy δ44/40Ca, δ26Mg, δ18O and δ13C approach

Sylvia Riechelmann, Vasileios Mavromatis, Dieter Buhl, Martin Dietzel, Adrian Immenhauser

Controls on formation and alteration of early diagenetic dolomite: A multi-proxy $\delta^{44/40}$Ca, δ^{26}Mg, δ^{18}O and δ^{13}C approach

Sylvia Riechelmann[a*], Vasileios Mavromatis[b,c], Dieter Buhl[a], Martin Dietzel[b] and Adrian Immenhauser[a]

[a] Ruhr-University Bochum, Institute of Geology, Mineralogy and Geophysics, Universitätsstraße 150, D-44801 Bochum, Germany

[b] Graz University of Technology, Institute of Applied Geosciences, Rechbauerstraße 12, 8010 Graz, Austria

[c] Géosciences Environnement Toulouse, CNRS, UMR 5563, Avenue Edouard Belin 14, 31400 Toulouse, France

[*]Corresponding author email address: Sylvia.Riechelmann@rub.de Tel. +49 (0)234 3225462

Compiled for: Geochimica et Cosmochimica Acta

Abstract

The full potential of the dolomite Ca isotope proxy only unfolds when combined with data of the other main elements (C, O, Mg) in the crystal lattice of Mg-carbonates. Data presented here reveal the level of complexity inherent to dolomite precipitation and alteration environments and add new constraints to the understanding of early diagenetic dolomite formation. Well-constrained Precambrian to Pleistocene dolomites were investigated, representing three characteristic formation and alteration environments: (i) sabkha, (ii) altered marine and (iii) lacustrine/palustrine dolomites. Primary sabkha dolomites with typically low cation ordering degree (COD), high $\delta^{13}C$ and low $\delta^{44/40}Ca$ values contrast with recrystallized sabkha dolomites with relatively high COD, low $\delta^{13}C$ and high $\delta^{44/40}Ca$ values. Both $\delta^{13}C$ and $\delta^{44/40}Ca$ values of sabkha dolomite bear witness to the relative effects of kinetic and equilibrium Ca isotope fractionation conditions. Primary sabkha dolomites display $\Delta^{44/40}Ca_{dolomite\text{-}fluid}$ ranging from -0.4 to -1.3‰, whereas recrystallized dolomite is approaching isotopic equilibrium ($\Delta^{44/40}Ca_{dolomite\text{-}fluid}$ ~0‰). Using the fractionation factor deduced from the sabkha dolomite data set, recrystallized Precambrian dolomite points to a $\delta^{44/40}Ca_{seawater/pore\ fluid}$ of about 1.2‰ (SRM 915a), a value that is distinctively lower compared to previously suggested ones for modern seawater. Altered marine dolomites display evidence for meteoric overprint, indicated by $\delta^{18}O$ values as low as -4.62‰. Both Mg and Ca isotope signatures correlate with $\delta^{18}O$ values of altered marine dolomites, whereas $\delta^{13}C$ values lack correlation with the other isotope systems. We propose that freshwater circulated through silicate aquifers prior to reaching the dolostone units and Ca, Mg and O isotopes of altered marine dolomites reflect variable degrees of this meteoric overprint. Lacustrine/palustrine dolomites display a correlation between the isotope values of C, Mg and Ca. These dolomites are formed during pulses of marine ingression in swamp, playa and lake environments and are thus characterized by water-logged conditions (anaerobic) and saline, sulfate-rich fluids. Bacterial-sulfate reduction induces dolomite formation and leads to lower $\delta^{13}C$ and $\delta^{44/40}Ca$ as well as to higher $\delta^{26}Mg$ values. The Ca isotope proxy acts as a benchmark against which other proxy data can be calibrated or processes tested. Taking COD and dolomite stoichiometry into consideration, the here documented multi-proxy isotope approach is promising and provides benchmarks against which proxy signals can be calibrated and tested. Interestingly, even the limited data sets shown here point to patterns that can be interpreted in a meaningful manner that is of relevance for dolomite research.

Keywords: Ca isotopes, dolomite, multi-isotope proxy approach

1. INTRODUCTION

Dolomite, $CaMg(CO_3)_2$, is a rock forming mineral, most prominent as dolostone, that consists of calcium and magnesium forming a double carbonate mineral. The cation ordering degree (COD) represents the order/disorder in the alternating layers of Mg and Ca in the crystal lattice of dolomite. Crystallographically, dolomite is defined by the 101, 015 and 021 `ordering´ reflections that are observed in the x-ray diffraction (XRD) pattern. These reflections are not present in the case of high-Mg calcite (5-30 mol% Mg) or very high-Mg calcite (> 30 mol% Mg) due to changes of the space group between dolomite ($R\bar{3}$) and calcite ($R\bar{3}c$). The substitution of Ca^{2+} ions by Mg^{2+} and *vice versa* can result in poorly ordered dolomite still representing the $R\bar{3}$ space group (Bradley et al., 1953; Gregg et al., 2015). Dolomite forms via direct mineral precipitation, as a diagenetic replacement phase, or as a pore-filling hydrothermal/metamorphic cement phase. In natural environments, dolomite is forming in a wide range of sedimentological, diagenetic and low-grade metamorphic settings (e.g., Land, 1973; Von der Borch et al., 1975; McKenzie, 1981; Kelts and McKenzie, 1982; Mazzullo et al., 1995; Meyers et al., 1997; Machel, 2004).

Sedimentary dolomites that form during an early diagenetic stage are usually calcian (>51 mol% Ca) in nature and often become partially or completely replaced by a later, more stable and more stoichiometric phase (molar Mg:Ca = 1:1; e.g., Land, 1982; Budd, 1997; Reeder, 1981, 1992). Moreover, the importance of dolomite precursor phases, referred to as very high-Mg calcite (VHMC), that may or may not alter to form poorly ordered dolomites has received significant attention (Gregg et al., 2015 *versus* Petrash et al., 2017). Although, dolomite is a major carbonate phase throughout Earth's history, Holocene stoichiometric dolomite precipitation in Earth's surface formation environments is a comparably rare process, and precipitation and alteration kinetics of dolomite are still not fully understood (e.g., Land, 1985, 1998; Chai et al., 1995). Owing to their complex nucleation and precipitation kinetics and volumetric significance in the geological record, dolomite minerals and dolostone rocks have been extensively studied using both field and laboratory approaches (e.g., Vasconcelos et al., 1995; Warren, 2000; Zhang et al., 2012; Geske et al., 2012, 2015a, b; Kell-Duivestein et al., 2019; Mueller et al., 2020).

Despite the fact, that Ca is a major element in dolomite, studies dealing with the calcium isotope signature ($\delta^{44/40}Ca$ or $\delta^{44/42}Ca$) of dolomite and dolostones were not common until recently, but their numbers have increased over the past few years (e.g., Jacobson and Holmden, 2008; Komiya et al., 2008; Holmden, 2009; Wang et al., 2012, 2014; Krause et al., 2012; Fantle and Higgins, 2014; Blättler et al., 2015; Higgins et al., 2018; Ahm et al., 2018, 2019; Jones et

al., 2020). In contrast, work documenting magnesium, carbon, oxygen and strontium isotope signatures of dolomite as well as major- and trace elemental concentrations (Ca, Mg, Sr, Mn, Fe) is far more common (e.g., Land, 1980; Vasconcelos et al., 1995; Malone et al., 1996; Machel, 2004; Bontognali et al., 2010; Pokrovsky et al., 2011; Geske et al., 2012, 2015a, 2015b; Mueller et al., 2020). In our view, Ca isotope data - in combination with other proxy data - have the potential to shed light on dolomite formation and alteration processes, and particularly so with respect to non-stoichiometric, Ca-rich dolomites, representing the bulk of early diagenetic dolomite throughout Earth's history (molar ratio of Mg:Ca < 1; e.g., Land, 1982).

Previous records compiled so far document that Ca isotope signatures of dolomite display a considerable variability and show distinct isotope fractionation patterns between fluid and primary or recrystallized dolomites. Primary dolomites, precipitated within siliciclastic sediments off the Peru continental margin and such related to cold seeps in the South China Sea, show an enrichment in ^{40}Ca relative to ^{44}Ca compared to the parent fluid ($\Delta^{44/40}Ca_{dolomite\text{-}fluid}$ from -0.4 to -0.7‰; Wang et al., 2012, 2014). Modelling of the isotope fractionation factor suggests an apparent $\Delta^{44/40}Ca_{dolomite\text{-}fluid} \approx$ -0.4‰ (Blättler et al., 2015). An even larger Ca isotope fractionation of between -1.0 and -1.1‰ ($\Delta^{44/40}Ca_{dolomite\text{-}fluid}$) was observed in the context of microbial dolomite culturing experiments (Krause et al., 2012). The discrimination against the ^{44}Ca *versus* the ^{40}Ca isotope, incorporated during divalent carbonate mineral formation, is probably indicative of kinetically controlled, mass-dependent Ca^{2+} ion diffusion, and/or preferential adsorption of the lighter ^{40}Ca onto growing carbonate mineral surface (Gussone and Dietzel, 2016 and references therein).

On the other hand, a $\Delta^{44/40}Ca_{dolomite\text{-}fluid}$ of about 0‰ is found for recrystallized dolomite (i.e., diagenetically altered mineral). This implies equilibrium conditions for Ca isotope fractionation between the solution and the carbonate mineral phase (cf., Jacobson and Holmden, 2008; Holmden, 2009; Gussone and Dietzel, 2016). Indeed, dolomite equilibration experiments at slightly elevated temperatures and calculations of Ca isotope fractionation factors for dolomite confirm a $\Delta^{44/40}Ca$ of about 0‰ at equilibrium conditions (Perez-Fernandez et al., 2017; Wang et al., 2017). Accordingly, an apparent Ca isotope fractionation factor between fluid and carbonate mineral close to 0‰ most likely reflects isotopic equilibrium conditions. This is typically the case when precipitation rates are very slow, whereas fast precipitation rates can result in precipitates that are depleted in the heavy isotope (e.g., Gussone and Dietzel, 2016).

Another factor that arguably influences Ca isotope fractionation is the temperature of the parent fluid. Calcite precipitation experiments document that fluid temperature has a

comparably weak influence on Ca isotope fractionation (about 0.02‰/°C), and hence, precipitation rate effects are considered more important (Lemarchand et al., 2004; Marriott et al., 2004; Gussone et al., 2005, Sime et al., 2005; Steuber and Buhl, 2006; Tang et al., 2008; AlKhatib and Eisenhauer, 2017). Both of these parameters, however, are not yet properly calibrated for dolomite formation.

Judging from the published literature available thus far, sedimentary dolomite Ca isotope ratios reflect: (i) (re)crystallization kinetics; (ii) the Ca isotope ratio of the source rock(s); (iii) the Ca isotope ratio of the parent fluid, and (iv) the degree of isotope exchange (and isotope fractionation) between fluid and mineral, fluid-rock interaction and the fluid-rock ratio (e.g., Tipper et al., 2008; Jacobson and Holmden, 2008; Komiya et al., 2008; Holmden, 2009; Holmden et al., 2012; Fantle and Higgins, 2014; Bradbury and Turchyn, 2018; Higgins et al., 2018; Ahm et al., 2018, 2019; Jones et al., 2020). The first studies combining evidence from Ca isotope data with Mg, C and O isotope data of dolomites are documented in Kasemann et al. (2005; 2014), Silva-Tamayo et al. (2010), Fantle and Higgins (2014), Blättler et al. (2015), Higgins et al. (2018), Ahm et al. (2018; 2019), and Jones et al. (2020). These authors report a co-variance within this quaternary (consisting of four) isotope system, in particular between Mg and Ca isotope signatures.

Here, we present $\delta^{44/40}$Ca values of a selection of well-constrained natural Precambrian to Pleistocene dolomites including: (i) sabkha dolomites, (ii) altered marine dolomites, and (iii) lacustrine/palustrine dolomites. The observed correlations between $\delta^{44/40}$Ca, δ^{26}Mg, δ^{13}C, δ^{18}O and cation ordering degree (COD) indicate that distinct correlations between these proxies reflect environmental and/or diagenetic conditions of dolomite formation. This study has three aims: First, we complement published data on dolomite calcium isotope signatures with new data measured from samples collected in Precambrian to Pleistocene outcrop belts worldwide. The wide range of sampling sites and sample ages contrasts previous studies making use of material from a single sampling locality, for example a core. Second, we assess, by means of Principal Component Analysis (PCA), the potential covariance within the quaternary isotope system (Ca, Mg, C and O) and consider cation ordering degree (COD) and dolomite stoichiometry. Third, we document and discuss to which degree this multi-proxy approach has potential to shed light on precipitation and alteration pathways of early diagenetic, non-stoichiometric dolomite.

This paper does not deal with the elusive topic of amorphous and very high-Mg calcites precursor phases and their bearing on isotope fractionation. Non-traditional crystallization pathways and metastable precursor phases most likely add further complexity but are best

explored in the context of experimental work (e.g., Gregg et al., 2015; Kell-Duivestein et al., 2019). We acknowledge that the present data set has limitations inasmuch as we cover a wide stratigraphic and environmental range with a limited number of data points. We are encouraged, however, by the fact that this data set shows relevant and important trends and we suggest future work to be based on this study. Data shown here have significance for those concerned with palaeoenvironmental reconstructions based on early diagenetic dolomite archives and the mineralogy and geochemistry of dolomites in general.

2. MATERIALS AND METHODS

2.1 Study material

A variety of well-characterized early diagenetic dolomites collected from locations worldwide were analyzed in the context of this study. In this paper, we apply the following terminology: (i) sabkha dolomite, (ii) altered marine dolomite, and (iii) lacustrine/palustrine dolomite (see Table S1 in Appendix A for details). Note, each data point represents a variable number of dolomite minerals drilled from one sample. This might imply that variations in the properties of individual dolomite minerals are averaged over the `bulk` sample. The attributes of many of the samples analyzed here are detailed in Geske et al. (2015a). We make use of these data where appropriate and particularly with reference to the cation ordering degree (COD) and carbon, oxygen and magnesium isotopic compositions. We would like to emphasize that all samples used here are crystallographic dolomite determined by means of X-Ray diffraction patterns (Appendix B; Geske et al., 2015a). Minerals other than dolomite were chemically removed prior to the sample analysis. For details on the sampling sites, age and analytical protocols refer to Appendix A and Geske et al. (2015a).

2.2 Sample preparation for calcium isotope analysis

Powdered samples that represent a poorly constrained admixture of both calcite and dolomite are treated with 0.27M Di-Na-EDTA to dissolve the calcitic phase following the method of Geske et al. (2015a, b). Samples containing anhydrite or gypsum were washed with deionized water to remove the sulfates. Between 0.07 to 0.15 mg of the dolomite powder was weighed, dissolved in 1 ml 6M HCl and then dried at 125°C on a hot plate. Subsequently, two different chemical separation techniques were applied. Half of the samples were dissolved in 1 ml 3M HNO_3 and Sr is separated from the remaining sample using TRISKEM Sr-Resin (100 –

150 mesh) and PFA columns. The residue was evaporated to dryness and 1 ml of a 1:1 mixture of H_2O_2:HNO_3 (31%:65%) was added to the dried samples to destroy organic compounds to avoid complexation of cations. Subsequently, samples were dried at 60°C and re-dissolved in 1 ml 2.5M HCl. The Ca fraction were separated using BioRad ion exchange resin AG50W-X12 (200 – 400 mesh) and quartz glass columns.

The other half of the samples was dissolved first in the H_2O_2:HNO_3 mixture and then dried before the sample was re-dissolved in 1 ml 2M HNO_3 to be prepared for the second separation technique. Here, a prepFAST MC (Elemental Scientific) machine equipped with a CF-MC-SrCa-1000 column was used for chemical separation. The matrix was washed out using 2M HNO_3, while in the next step Sr is removed with 10 ml 5M HNO_3. The Ca fraction was gained with 5 ml 0.1M HCl. The recovered Ca fraction of both separation techniques was dried on a hot plate and re-dissolved in 3.5% HNO_3.

A 3 ppm solution was prepared for Ca isotope analysis using a Thermo Fisher Scientific Neptune MC-ICP-MS in the laboratory of the Sediment and Isotope Department at Ruhr University Bochum. The standard sample bracketing technique was applied to calculate $\delta^{44/42}$Ca and the subsequent standard solution used is IAPSO seawater, which was separated from its matrix elements. Each sample was measured five times with each cycle comprising 30 measurements resulting in a total of 150 values. The reproducibility of Ca isotope measurements was validated using the standards (i) SRM-915a and (ii) USGS EN-1. Both separation techniques are used and the calcium isotope measurements of SRM-915a resulted in $\delta^{44/42}$Ca = -0.99‰ ± 0.09 2σ and $\delta^{44/43}$Ca = -0.45‰ ± 0.07 2σ (n = 79; traditional column chemistry) and in $\delta^{44/42}$Ca = -0.97‰ ± 0.06 2σ and $\delta^{44/43}$Ca = -0.43‰ ± 0.03 2σ (n = 20; prepFAST MC). Measurements of EN-1 show values of $\delta^{44/42}$Ca = -0.55‰ ± 0.07 2σ and $\delta^{44/43}$Ca = -0.25‰ ± 0.06 2σ (n = 5; traditional column chemistry) and $\delta^{44/42}$Ca = -0.54‰ ± 0.07 2σ and $\delta^{44/43}$Ca = -0.31‰ ± 0.06 2σ (n = 4; prepFAST MC). These results are in agreement with values reported previously (e.g., Wieser et al., 2004; Steuber and Buhl, 2006; Ryu et al., 2011; Hippler et al., 2013).

For comparison of the Ca isotope values with previous studies, the $\delta^{44/42}$Ca values are converted into $\delta^{44/40}$Ca values via the equation by Heuser et al. (2016) assuming mass dependent fractionation.

$$\delta^{44/40}Ca \approx \delta^{44/42}Ca * \frac{\ln (m^{44}Ca/m^{40}Ca)}{\ln (m^{44}Ca/m^{42}Ca)} \quad (1)$$

with m^xCa representing the atomic mass of each Ca isotope. In order to convert the standard IAPSO into SRM 915a the following equation was used (Heuser et al., 2016):

$$\delta^{44/40}Ca_{SRM\ 915a} = \delta^{44/40}Ca_{IAPSO} + 1.88 \quad (2)$$

2.3 Data analysis

In order to determine the relations between the quaternary isotope system and the COD, correlation coefficients are calculated using the Pearson-correlation (*r*). The *p-value* is given to validate the significance of a correlation with $p < 0.05$ (95% significance level) indicating a statistically significant correlation. Principal Component Analysis (PCA; von Storch and Zwiers, 2002; Navarra and Simoncini, 2010) was performed with the standardized data using the software PAST3 (Hammer et al., 2001) to identify proxies driven by the same factor.

3. RESULTS

3.1 Calcium isotope data

Sabkha dolomites display the highest variability in their Ca isotopic composition ranging between 0.37‰ and 1.19‰ ($\delta^{44/40}Ca_{mean}$: 0.74 ± 0.48‰ 2σ, n = 13). Altered marine dolomites range from 0.58‰ to 0.92‰ ($\delta^{44/40}Ca_{mean}$: 0.76 ± 0.31‰ 2σ, n = 4), and lacustrine/palustrine dolomites vary between 0.55‰ and 0.91‰ ($\delta^{44/40}Ca_{mean}$: 0.69 ± 0.27‰ 2σ, n = 8; Table 1 and Fig. 1). Calcium isotope values of all three dolomite types overlap and display similar mean values. Two types of lacustrine/palustrine dolomites were analysed: (i) Palustrine dolomites (i.e. the `coal ball dolomites´ described in Richter et al. 2014 and references therein) having lowest $\delta^{44/40}$Ca values, and (ii) playa and lake dolomites, which show Ca isotope ratios that are moderately enriched in the heavy isotope (Table 1).

3.2 Four-fold (quaternary) isotope approach and cation ordering degree of dolomite

Sabkha dolomites yield positive δ^{13}C values with a mean of +3.27 ± 2.18‰ 1σ and a wide range in the cation ordering degree (COD; 0.21 – 0.93; Fig. 2A and Table 1). Sabkha dolomites with a higher COD have ^{13}C depleted values and *vice versa*. The correlation between δ^{13}C values and the COD, however, is weak ($r = -0.47$, $p = 0.10$, $n = 13$; Fig. 2A). Altered marine dolomites display δ^{13}C values between +3.01 and -0.57‰ and the highest COD (0.84 – 1.00; Fig. 2A and Table 1). They display the same trend as observed in sabkha dolomites ($r = -0.82$, $p = 0.18$, $n = 4$; Fig. 2A). Lacustrine/palustrine dolomites display the lowest δ^{13}C values (-22.10

to -1.43‰), with coal ball dolomites at the ^{13}C depleted end of the spectrum and lake dolomite at the ^{13}C enriched end of the spectrum (Fig. 2A and Table 1). The COD ranges between 0.36 – 0.67 (Fig. 2A and Table 1). In contrast to sabkha and altered marine dolomites, a positive correlation between COD and $\delta^{13}C$ values is observed (Fig. 2A).

Sabkha dolomites display higher $\delta^{44/40}Ca$ values with increasing COD resulting in a significant positive correlation. With reference to altered marine dolomites (Fig. 2B and Table 1), no obvious pattern is observed. Lacustrine/palustrine dolomites show a significant positive correlation between $\delta^{44/40}Ca$ and COD (Fig. 2B and Table 1).

Carbon and $\delta^{44/40}Ca$ isotope data of sabkha dolomites correlate negatively on a significant level with decreasing Ca isotope ratios linked to increasing $\delta^{13}C$ values (Fig. 2C and Table 1). No correlation between Ca and C isotope values is observed for altered marine dolomites (Fig. 2C). On the other hand, lacustrine/palustrine dolomites display increasing $\delta^{44/40}Ca$ values with increasing $\delta^{13}C$ values, thus a significant positive correlation is observed (Fig. 2C and Table 1).

Magnesium isotope values of sabkha dolomites range between -2.49 and -1.67‰, whereas altered marine dolomites show weakly ^{26}Mg-enriched values (-1.86 to -1.10‰; Fig. 3 and Table 1). In case of both dolomite types, no significant relation of Mg isotope ratios with $\delta^{13}C$ values could be observed (Fig. 3A). In contrast, $\delta^{26}Mg$ and $\delta^{13}C$ values of lacustrine/palustrine dolomites correlate negatively on a significant level (Fig. 3A and Table 1). Coal ball dolomites display the highest $\delta^{26}Mg$ values (Fig. 3). When comparing $\delta^{26}Mg$ with $\delta^{44/40}Ca$ values, only lacustrine/palustrine dolomites display a significant negative correlation. Altered marine dolomites and sabkha dolomites $\delta^{26}Mg$ and $\delta^{44/40}Ca$ show no obvious correlation at all (Fig. 3B).

Altered marine dolomites display comparably ^{18}O-depleted values from -4.62 to -3.50‰ (Fig. 4 and Table 1). A positive correlation is found when plotting $\delta^{18}O$ *versus* $\delta^{44/40}Ca$ and a negative one for $\delta^{18}O$ *versus* $\delta^{26}Mg$ (Fig. 4). Both correlations are close to the 2σ significance level ($p < 0.05$) but the data set is small (four data points). No significant correlations between Ca, Mg, C, and O isotope values is observed for sabkha and lacustrine/palustrine dolomites (Figs. 4 and 5).

Principal component analysis of the five proxies of each dolomite type support the observations provided by the Pearson correlations (Fig. 5, Table 2). It has to be kept in mind that both Pearson correlations and Principal component analysis evaluate linear relations in contrast to non-linear relations. In the case of the data set documented here, linear relations represent the best fit. In case of sabkha dolomites, variations in the COD, $\delta^{13}C$, $\delta^{18}O$ and

$\delta^{44/40}$Ca are mainly driven by one factor (PC 1; Fig. 5A, Table 2). On the other hand, δ^{26}Mg is mainly driven by another factor (PC 2), which has a weak influence on COD and δ^{13}C, but virtually no influence on δ^{18}O and $\delta^{44/40}$Ca (Fig. 5A, Table 2). Oxygen isotope signatures, δ^{26}Mg and $\delta^{44/40}$Ca of altered marine dolomite form a group and variations are driven by the same factor (PC 1; Fig. 5B, Table 2). Cation ordering degree and δ^{13}C, however, are mainly influenced by a second factor (PC 2, Fig. 5B, Table 2). Variations of COD, δ^{13}C, δ^{26}Mg and $\delta^{44/40}$Ca of lacustrine/palustrine dolomites are dependent on one component (PC 1). In any case, δ^{13}C seems to be influenced by a second factor driving the variations in δ^{18}O (PC 2; Fig. 5C, Table 2).

4. INTERPRETATION AND DISCUSSION

Calcium isotope ratios of Precambrian to Pleistocene dolomites presented in this study plot in the same range as previously published Ca isotope data of dolomites (Fig. 1). Moreover, Ca isotope signatures of marine dolomites documented in the literature are similar in range with sabkha dolomite Ca isotope data shown here, suggesting comparable formation processes or fluid Ca isotope composition (Fig. 1). We thus conclude that our samples and the data obtained from these samples are representative. Early burial, hydrothermal and methanogenic and some of the marine dolomites are most notably enriched in the heavier Ca isotope as exemplified in Neoproterozoic marine dolomites (Kasemann, et al., 2005; 2014; Komiya et al., 2008; Silva-Tamayo et al., 2010; Ahm et al., 2019). Dolomite associated with sulfate reduction and brine reflux show an enrichment in the lighter Ca isotope.

4.1 `Bulk´ sabkha dolomites

The sabkha depositional environment is characterized by high degree of evaporation of seawater, particularly during low tide, and intense microbial activity resulting in cm`s thick biofilms (Bontognali et al., 2010) in the intertidal sabkha environment. Calcian dolomite and very high-Mg calcite precipitation and ripening takes place during very shallow marine porewater burial (1-2 m) and is often most pronounced in sedimentary layers rich in organic matter (Bontognali et al., 2010; Geske et al., 2015b). These organic-rich layers probably represent buried microbial mats. This environment of dolomite formation is characterized by (i) high Mg/Ca ratios of the evaporated seawater, (ii) bacterial sulfate reduction and methanogenesis and (iii) elevated pore fluid temperatures up to about 30 °C (e.g., Morse, 2005; Nichols, 2009).

Here, we deal with fossil `bulk´ dolostone samples, the typical archive material used in palaeoceanographic studies. The Pleistocene, Mesozoic, Palaeozoic and Proterozoic sabkha dolostone samples shown here (Appendix A Table S2), yield dolomite minerals with a range of ordering from 0.21 to 0.93, typical for many recrystallized, formerly early diagenetic dolomites (Table 1; Geske et al., 2015a). There is no clear relation between the cation ordering degree and the age of the sample, suggesting that burial depth and other parameters are instrumental (Geske et al., 2012). With reference to (sub-)recent sabkha dolomites, Geske et al. (2015b) documented that very high-Mg calcites, poorly-ordered (but near-stoichiometric) as well as well-ordered dolomites co-exist at the same stratigraphic level in shallow cores. Clearly, this reflects the complexity of the system and the reason for this is, in the view of the authors, not well understood. In the fossil samples dealt with here, the variability in the COD of the individual dolomite minerals that are lumped into one sample is likely less pronounced. In order to understand the implications of the data shown here, it is relevant to follow the diagenetic evolution of the fossil `bulk´ dolomite samples discussed. Evidence for this comes from the study of recent sabkha environments and petrographic and geochemical data.

We argue that during their formation, the majority of dolomites in these samples precipitated as very high-Mg calcite precursor phases or as non-stoichiometric, poorly ordered to ordered dolomites (see discussion in Gregg et al., 2015 *versus* Petrash et al., 2017). This is supported by the high COD for at least some of the dolomites found in buried (sub-)recent microbial mats in the Abu Dhabi sabkha (Geske et al., 2015b). Bontognali et al. (2010) argued that dolomite (or very high-Mg calcite) formation in sabkha environments takes place in both: (i) the active microbial mat at the sediment surface and (ii) the inactive microbial mat during burial. In the first case, seawater represents the parent fluid. The geochemistry of these very early diagenetic dolomites is likely affected—at least to some degree—by mineral precipitation rates and/or biological effects. Triggered by reaction kinetics, the variously-ordered diagenetic dolomite minerals in a given `bulk´ sample will ripen and undergo geochemical re-equilibration during shallow burial marine pore fluid diagenesis and then gradually equilibrate with their ambient fluids (Geske et al., 2015a). The evaporated marine pore fluids will deviate to some degree from the geochemistry of the open marine seawater.

The $\delta^{13}C$ values of the ancient `bulk´ sabkha dolostone samples clearly point to a marine dissolved inorganic carbon (DIC) source. Similar $\delta^{13}C$ values are observed for modern carbonate platform sediments (Lowenstam and Epstein, 1957; Milliman, 1974, McKenzie, 1981). Further evidence comes from the typically marine Sr concentrations of these dolomites with a mean Sr concentration of 147 ppm (Geske et al., 2015a). Generally, the Sr concentration

of the sabkha dolomites ranges from 20 to 168 ppm (note, one sample has a Sr concentration of 595 ppm; Kri; Geske et al., 2015a). Previous studies documented that the Sr concentrations of dolomite scatter around 100 ppm, when the Sr/Ca_{fluid} ratio is close to seawater (Vahrenkamp and Swart, 1990). Thus, we conclude that the here analysed sabkha dolomites precipitated from seawater or altered marine pore fluids as suggested in previous studies (e.g., Land, 1980; Machel and Anderson, 1989; Budd, 1997; Swart et al., 2005). Higher Sr concentrations of dolomites can be generated when the Sr/Ca_{fluid} ratio increases due to recrystallization of carbonate minerals, gypsum or anhydrite (Swart et al., 2005). This pattern might explain the increased Sr concentration of dolomite sample Kri. Evidence comes from x-ray diffraction patterns of the untreated sample displaying anhydrite as additional mineral phase (see Appendix B – Kri).

Decreasing $\delta^{13}C$ values of the dolomite samples coincide with increasing COD (recrystallization; Fig. 2A) and point to micro-scale dissolution-re-precipitation processes approaching isotopic equilibrium conditions in respect to seawater or altered marine pore fluids (McKenzie, 1981; Warren, 2000). Pore fluids tend to have ^{13}C-depleted DIC values, relative to open oceanic seawater, due to microbial activity (Bontognali et al., 2010). Both, COD and $\delta^{13}C$ values, are influenced in a comparable manner by two components as observed in the PCA, with PC 1 having a higher influence relative to PC 2 (Fig. 5A and Table 2). Consequently, we propose that $\delta^{13}C$ values and COD of sabkha dolomites are mainly a function of the ratio of kinetic *versus* equilibrium conditions (PC 1) and, to a lesser degree, influenced by microbial activity (growth kinetics; PC 2). Other parameters such as fluid temperature and precipitation of other carbonate-bearing minerals might be relevant too.

Both the Pearson correlation and PCA display a relation between $\delta^{44/40}Ca$ and both cation ordering degree and $\delta^{13}C$ values of sabkha dolomites (Figs. 2B, C, 5A and Table 2). We propose that all of these attributes are interrelated and that $\delta^{44/40}Ca$ values are more strongly influenced by PC 1 (ratio of kinetic *versus* equilibrium conditions or rather unaltered *versus* recrystallized dolomites) compared to microbial metabolism (PC 2; Fig. 5A and Table 2). Early diagenetic, calcian sabkha dolomites are enriched in ^{40}Ca relative to their parent fluid (considering modern $\delta^{44/40}Ca_{seawater}$ = 1.88‰ SRM 915a; Fig. 2B). This observation is in agreement with previously reported $\Delta^{44/40}Ca_{dolomite\text{-}fluid}$ of -0.4 to -0.7‰ reflecting precipitation rate (Fantle and DePaolo, 2007; Jacobson and Holmden, 2008; Tang et al., 2008; Wang et al., 2012; 2014; Blättler et al., 2015; Gussone and Dietzel, 2016).

Fluid temperatures might also kinetically affect $\delta^{44/40}Ca_{dolomite}$ via increased precipitation rates, but this process is poorly constrained. The temperature difference of shallow

burial (0.3-0.5 m) marine pore fluids between winter and summer months in the actualistic sabkha environment of Abu Dhabi is in the order of 20 °C (Lokier et al., 2013). This range translates into a temperature-induced difference of about 0.1‰ for $\delta^{44/40}Ca$ (Rustad et al., 2010). This difference is smaller than the range of Ca isotope ratios of sabkha dolomites observed here (0.83‰; Table 1).

Considering effects of growth kinetics on Ca isotope fractionation between dolomite and precipitating solution (Fig. 5A), calcian, poorly ordered dolomites represent a (semi-qualitative) archive of the Ca isotope signature of their parent fluid (here evaporated marine pore fluid). In the sense of a tentative working hypothesis, the mean Ca isotope seawater curve of Farkaš et al. (2007) is used for estimating $\Delta^{44/40}Ca_{dolomite\text{-}fluid}$. Note, Farkaš et al. (2007) use a constant fractionation factor between calcite and parent solution. Keeping the latter simplification in mind, a $\Delta^{44/40}Ca_{dolomite\text{-}fluid}$ between -0.4 and -1.3‰ for early diagenetic sabkha dolomite is obtained. This values are in reasonable agreement with the kinetic Ca isotope fractionation factors proposed in the literature ($\Delta^{44/40}Ca_{dolomite\text{-}fluid}$ of -0.4 to -0.7‰; Fantle and DePaolo, 2007; Wang et al., 2012, 2014; Blättler et al., 2015; Gussone and Dietzel, 2016). The observed range in isotope fractionation factors, however, exceeds values typically found in the literature ($\Delta^{44/40}Ca_{dolomite\text{-}fluid}$ up to -1.3‰). This observation suggests that kinetic isotope effects are relevant during precipitation (Fig. 5A). Note, the kinetic control of $\Delta^{44/40}Ca_{dolomite\text{-}fluid}$ between -1.0 and -1.1‰, as reported in Krause et al. (2012), is in close agreement with the reconstructed $\Delta^{44/40}Ca_{dolomite\text{-}fluid}$ of up to -1.3‰ for early diagenetic sabkha dolomites as proposed here.

Fossil, recrystallized, formerly calcian dolomites that experience isotopic equilibration, are likely reflecting the Ca isotopic composition of their parent fluid (e.g., Jacobson and Holmden, 2008; Holmden 2009; Perez-Fernandez et al., 2017; Wang et al., 2017). Early diagenetic recrystallization, however, results in isotopically more heavy Ca isotope signatures (approaching the fluid Ca isotope composition) relative to the dolomite minerals at formation (Fig. 2B). This pattern is reflected in a reduced value of the isotope fractionation factor between the solid and the fluid from -0.7 in primary samples to 0‰ in recrystallized dolomites (e.g., Jacobson and Holmden, 2008; Holmden 2009; Wang et al., 2012,2014; Blättler et al., 2015; Gussone and Dietzel, 2016). Similar patterns were reported for the $\delta^{44/40}Ca$ values of limestone (Fantle and Higgins, 2014) and for dolomitized limestone (Higgins et al., 2018). The dolomite sample with the highest cation ordering degree representing the most recrystallized dolomite (COD 0.93, Angola 1; Table 1) has a $\delta^{44/40}Ca$ value of 1.19 ± 0.12‰. Assuming a $\Delta^{44/40}Ca_{dolomite\text{-}seawater}$ of 0‰, the $\delta^{44/40}Ca_{Angola1}$ equals the $\delta^{44/40}Ca_{seawater}$ value, which, along

these lines of reasoning, translates in a Precambrian (Neoproterozoic) seawater (or better marine pore fluid) Ca isotope signature of 1.19‰. Clearly, any sophisticated interpretation of this limited data set must be avoided. Nevertheless, it is of interest that this value is depleted in ^{44}Ca compared to the modern seawater Ca isotope signature (1.88‰ SRM 915a) and also depleted relative to the Phanerozoic portion of the Ca isotope seawater curve of Farkaš et al. (2007). Prior to the advent of biomineralization near the Precambrian-Cambrian boundary, a pronounced biogenic effect on seawater Ca-isotope signatures seems unlikely. Nevertheless, the significance of microbial and algal metabolism on seawater Ca isotope signatures must not be neglected. Throughout the Phanerozoic, the seawater Ca isotopic composition is clearly affected by long-term patterns in marine biomineralization among which the evolution of calcareous planktonic organisms in the Mesozoic (Stanley and Hardie, 1998) is but one factor.

Although Ca isotope ratios, C isotope ratios and the cation ordering degree of sabkha dolomites display clear relations, $\delta^{26}Mg_{sabkha\ dolomite}$ values lack a relation (linear or non-linear) with any of the other parameters (Figs. 3, 4B and 5A). It seems that the parameters (or the degree thereof) affecting $\delta^{26}Mg_{sabkha\ dolomite}$, differ from those affecting Ca and C isotopes and cation ordering. Blättler et al. (2015) present variations of C, Mg and Ca isotopes of authigenic dolomite nodules formed within siliciclastic sediments below the seafloor. Isotope variations documented are set in relation to pore fluid variations due to bacterial sulfate reduction and methanogenesis. Both of these processes influence dolomite precipitation in sabkha environments (e.g., Morse, 2005; Nichols, 2009). Carbon and calcium isotope ratios of less-ordered, calcian sabkha dolomite data shown here display an anti-correlation similar, but less pronounced, to that observed by Blättler et al. (2015). This feature, in combination with the PCA, confirms that $\delta^{44/40}Ca$ and $\delta^{13}C$ are mainly controlled by the ratio of kinetic *versus* equilibrium conditions (PC 1), and to a lesser degree by microbial metabolism (PC 2; Fig. 5A and Table 2). In contrast, PC 2 of the principal component analysis (microbial activity) has a strong influence on $\delta^{26}Mg$ values (Fig. 5A and Table 2) with variations of 0.82‰ or less (Figs. 3 and 5A). The degree of microbial activity might be responsible for the wide range $\delta^{26}Mg$ values. Alternatively, $\delta^{26}Mg_{sabkha\ dolomite}$ represent the Mg isotopic composition of the isotopically altered marine pore fluid during recrystallization. Fluid alteration with increasing burial depth goes hand in hand with the precipitation of Mg-bearing minerals other than calcian dolomite (Geske et al., 2015a, b). Magnesium is possibly buffered by the initially high concentrations in seawater but the Mg isotope signatures seem unrelated to recrystallization (PC 1; Fig. 5A). Nevertheless, it cannot be excluded completely that recrystallization has an

influence. Albeit in in a non-linear manner, on the Mg isotope signature of sabkha dolomites. Evidence for this, however, might be overprinted by other more dominant processes.

Concluding, both the $\delta^{13}C$ and the $\delta^{44/40}Ca$ values of sabkha dolomites reflect patterns that are best explained by an initial precipitation as metastable very high-Mg calcite and non-stoichiometric (calcian) dolomites followed by subsequent crystallographic and geochemical ordering to form more stoichiometric, better-ordered dolomite (Geske et al., 2015b; Figs. 2C, 5 and 6). Complexity arises as some of these microbiologically-mediated precipitates may form via amorphous precursor phases (Petrash et al., 2017). This pathway reflects both, initial kinetics (precipitation rate, microbial activity) and subsequent isotopic near-equilibrium fractionation with marine pore fluid. Under the condition that the ambient pore fluid is still largely representative of seawater, these early diagenetic and recrystallized dolomite $\delta^{44/40}Ca$ values have potential as (relative) proxies for patterns in marine pore fluid evolution through geological time. Given the remarkable complexity of these systems, we, however, discourage sophisticated statements regarding `absolute´ palaeo-seawater $\delta^{44/40}Ca$ values based on these archives.

4.2 `Bulk´ altered marine dolomite

Here, the term `altered marine dolomite´ refers to Mg carbonates that precipitated from seawater but then underwent subsequent alteration in the presence of non-marine (often meteoric) fluids as indicated by the low oxygen isotopic composition ($\delta^{18}O_{mean}$ = -4.2‰; Fig. 4; Geske et al., 2015a). This overprint resulted in recrystallization, an observation that is further supported by the high COD (0.84 – 1; Table 1 and Fig. 2A, B). Similar to the sabkha dolomites, the carbon source of $\delta^{13}C_{altered\ marine\ dolomites}$ values is seawater (Geske et al., 2015a), implying a rock buffered system for the element carbon and a non-marine fluid that carries only low amounts of dissolved inorganic carbon. When the non-marine fluid dissolves the host limestone aquifer, the marine signature is taken up and shifts the fluid $\delta^{13}C$ values towards the marine end-member. Only a weak relation between COD and the $\delta^{13}C$ values of the altered marine dolomites is found (Fig. 2A). The PCA implies that the COD and the dolomite $\delta^{13}C$ values mainly respond to the same process—most likely recrystallization (Fig. 5B; Table 2). When plotting the Ca or Mg isotopic composition against the COD or carbon isotope signatures, respectively no statistically relevant correlation occurs as confirmed by PCA (Figs. 2B, C, 3A, 5B and Table 2).

Calcium and Mg isotope ratios correlate with $\delta^{18}O$ values (Figs. 4 and 5B). This might imply that both of these elements (and their isotopes) respond to meteoric waters in a fluid-

buffered system. This is further supported by PCA, implying that one factor drives most of the variations shown in O, Mg and Ca isotope ratios (Fig. 5B and Table 2). Altered marine dolomites analysed here have Sr concentrations ranging between 7 and 54 ppm (Geske et al., 2015a). According to Swart et al. (2005), dolomites overprinted by a non-marine fluid can be distinguished from other dolomites by their lower Sr concentrations. This is either due to the precipitation of Sr-bearing minerals, a hypothesis that can be excluded due to the lack of non-dolomite minerals in the sample (see Appendix B), or due to mixing of calcium-rich freshwater with seawater resulting in a low Sr/Ca ratio fluid (Swart et al., 2005).

Samples with ^{18}O-depleted values display a higher degree of meteoric alteration and have lower $\delta^{44/40}$Ca and higher δ^{26}Mg values. Meteoric waters (soil-, aquifer or riverine/lacustrine fluids) display considerable variability in their Ca and Mg isotopic composition depending on climate, bedrock lithology and fractionation during water-rock interactions. Generally, waters in rivers and in aquifers have low Ca isotope values compared to seawater (e.g., Holmden et al., 2012). Higher Ca isotope ratios are observed for water percolating through carbonate host rock and lower values for water interacting with silicate bedrock (Walter et al., 2015; Tipper et al., 2016). With respect to Mg isotope signatures, fluids percolating through a carbonate host rock have lower δ^{26}Mg values, whereas higher values are found for rivers draining silicate hinterlands (Teng, 2017). Judging from the high COD, the calcium isotope fractionation factor for recrystallized dolomites is suggested to oscillate around 0‰. With reference to the two dolomite samples with degrees of order > 0.9, this may imply that the $\delta^{44/40}$Ca values of the meteoric fluids that induced alteration range between 0.92 and 0.69‰ (Table 1). These values agree well with the mean $\delta^{44/40}$Ca value of rivers draining silicate hinterlands (0.85 ± 0.03‰; 2SE; Tipper et al., 2016). This is further supported by the δ^{13}C values, which lack an overprint with HCO_3^- rich water as induced by dissolution of carbonate rocks. With regard to PCA (Fig. 5B and Table 2), both δ^{18}O and $\delta^{44/40}$Ca are moderately influenced by PC 2, most likely recrystallization. This is not the case for the Mg isotope composition (Fig. 5B and Table 2). Given that PCA analysis evaluates linear relations only, it might be possible that the Mg isotope composition of the altered marine dolomites is affected by recrystallization in a non-linear manner. This feature, however, is difficult to test with the data presented here and requires more work.

Additional information is found in the $\delta^{26}Mg_{\text{altered marine dolomite}}$ values, which are enriched in ^{26}Mg (Fig. 4). This might suggest that the meteoric diagenetic fluids carry silicate bedrock Mg isotopic signatures. Alternatively, meteoric fluids, depleted in Mg, leached the light Mg isotope from the dolomite during the recrystallization process. This would then lead to higher

bulk dolomite δ^{26}Mg values. This scenario was experimentally confirmed for biogenic low-Mg calcite exposed to meteoric fluids (Riechelmann et al., 2016; 2018). Rayleigh-type distillation offers an alternative explanation. Although the light isotope (^{24}Mg) is preferentially incorporated into dolomite minerals (negative fractionation), the heavier isotope (^{26}Mg) will also be increasingly incorporated in a Mg-limited system. If this holds true, then the meteoric fluid was Mg-lean.

The trend between Ca and Mg isotope signatures of altered marine dolomites, although statistically not significant (Fig. 3B), might suggest that: (i) one of the two isotope systems is more sensitive to meteoric diagenetic overprint compared to the other one, (ii) the initial Ca isotope signatures of the marine dolomite was close to that of the diagenetic fluid, or (iii) the processes driving Ca and Mg isotope variations of altered marine dolomites differ (Ca-rich *versus* Mg-poor meteoric fluid, recrystallization *versus* dissolution; Fig. 4). An alternative and perhaps more straightforward interpretation is that the four samples (Moggast1, Hund1, Contrin2, Prüstr. 4; Table 1) were collected at different sampling sites in Germany and Italy (Table S2 in Appendix A). Diagenetic (meteoric) fluids, interacting with different host lithologies at each site, most likely differed in their (isotope) geochemistry. This simple observation represents a warning to not uncritically lump data from samples that have been collected at different locations. Generally, altered marine dolomite data shown here are from four samples only. Nevertheless, the correlations displayed in figure 4 are close to the significance level ($p < 0.05$) and the trends observed seem valid verified by PCA (Fig. 5B and Table 2). Clearly, the compilation of a more substantial data set is required to test the above hypotheses.

Summing up, δ^{18}O, $\delta^{44/40}$Ca and δ^{26}Mg signatures of altered marine dolomites reflect fluid-buffered diagenesis (Fig. 6). Conversely, the δ^{13}C of these dolomites is in agreement with a rock-buffered system. Clearly, it must be kept in mind that a diagenetic system might be fluid-buffered with respect to one element and rock-buffered with respect to another element. Calcium isotope signatures of altered marine dolomites carry the $\delta^{44/40}$Ca signature of the reactive fluid and bear important information on the mineralogy of the aquifer rock (Fig. 6). Concluding, on the level of a working hypothesis, altered marine dolomites represent fair archives of temporal patterns in seawater geochemistry.

4.3 `Bulk´ lacustrine/palustrine dolomites

Palustrine dolomites (referred to as `coal balls´ in the literature; Richter et al., 2014 and references therein) formed in an ancient coastal marsh environment experiencing transient

559 marine ingressions. During transgressive events, seawater carried dissolved Mg into the
560 palustrine environment inducing dolomite precipitation (Geske et al., 2015a). This peculiar
561 depositional environment was characterized by abundant organic plant material and anaerobic
562 microbial processes. Seawater ingressions and plant material provided the base for sulfate-
563 reducing bacteria in the upper sedimentary column, whereas bacterial oxidation might have
564 dominated the near-surface layers (e.g., Orem and Finkelman, 2005; Nichols, 2009). It remains
565 at present debated, if the removal of sulfate from the ambient fluid can lead to an increase in
566 alkalinity and result in precipitation of carbonate minerals (e.g., Baker and Kastner, 1981;
567 Warren, 2000). Previous work suggested that in such an environment, non-stoichiometric
568 dolomites formed rapidly as these minerals entomb extremely well preserved plant remains that
569 have not yet seen decay (e.g., Zhou et al., 2008). All of these observations agree with the low
570 cation ordering degree of these dolomites (0.36-0.39; Table 1 and Fig. 2A, B), indicative of
571 their early diagenetic, non-stoichiometric nature.
572 Playa and lake dolomite analyzed in the context of this study arguably precipitated from
573 saline to hypersaline Mg-rich groundwater in a continental environment (Geske et al., 2015a).
574 Following previous workers, we assume that the playa lake was characterized by a restricted
575 water circulation, exhibited a stratified water column due to the high salinity of the lake water
576 and was recharged by groundwater only (e.g., Nichols, 2009). For both, playa and saline lake
577 dolomites, an anaerobic formation environment is assumed. The saline groundwater that
578 recharged the playa and the lake environment provided sulfate, which arguably led to a bloom
579 of sulfate-reducing bacteria (e.g., Nichols, 2009). Although the COD of playa (0.67) and lake
580 (0.52) dolomite is higher than that of palustrine dolomite, they probably formed as very early
581 diagenetic precipitates (Geske et al., 2015a). Given the rather peculiar, and only in part
582 comparable diagenetic environments of palustrine, lake and playa dolomites, these minerals
583 display no significant relation between their COD and $\delta^{13}C$ signatures (Fig. 2A). The strongly
584 ^{13}C-depleted isotope ratios of palustrine dolomites point to the presence of isotopically low
585 organic matter and the influence of bacterial sulfate-reduction (Table 1 and Fig. 2A, C; e.g.,
586 Claypool and Kaplan, 1974; Machel et al., 1995; Blättler et al., 2015; Geske et al., 2015a).
587 Extracellular polymeric substance (EPS) can act as a substrate for dolomite formation
588 (Krause et al., 2012). Due to the accumulation of the isotopically light Ca isotopes by EPS
589 (Mavromatis et al., 2012; Krause et al., 2012), Ca isotope signatures of dolomites shift to lower
590 values in the presence of sulfate-reducing bacteria. Bradbury et al. (2020) observed a similar
591 trend for experiments precipitating calcite in the presence of *Desulfovibiro bizertensis*. These
592 authors recognized an increase in Ca isotope fractionation with increasing bacterial activity

(Bradbury et al., 2020). Along these lines, Krause et al. (2012) suggests that the Ca isotope composition of dolomites is strongly dependent on pre-fractionation by microbial activity rather than of fractionation between the ambient fluid and the dolomite.

Principal component analysis indicates that Ca, Mg and C isotope composition of lacustrine/palustrine dolomites are influenced by the same factor (Fig. 5C and Table 2), which we believe to be microbial sulfate-reduction. In experiments involving sulfate-reducing bacteria in order to facilitate dolomite precipitation, Krause et al. (2012) found an offset of $\Delta^{44/40}Ca_{dolomite\text{-}fluid}$ between -1.0 to -1.1‰. Applying this to the data presented here, $\delta^{44/40}Ca$ values of 1.55 to 1.84‰ result for palustrine fluids, values of 1.85 to 1.95‰ are found for saline lake and values of 1.91 to 2.01‰ seem typical for playa waters. These results fall within the range of $\delta^{44/40}Ca_{groundwater}$ (0.17 to 2.08‰; $\delta^{44/40}Ca_{mean} = 0.86 \pm 0.10$‰ 2SE, n = 65; Tipper et al., 2016) and are also very close to the measured mean $\delta^{44/40}Ca_{seawater}$ value of 1.89 ± 0.02 (2SE, n = 62; Tipper et al. 2016). Nevertheless, we hypothesize that various bacterial consortia were probably most active in the organic-rich marsh environments but different consortia were active in playa and saline lake environments. This is further supported by the observation that increased bacterial activity leads to increased Ca isotope fractionation (Bradbury et al., 2020). If this holds true, then the lower $\delta^{44/40}Ca$ and $\delta^{13}C$ data of palustrine dolomites and the higher values for playa and lake dolomite are reasonably explained (Fig. 6).

Blättler et al. (2015) found a correlation between dolomite carbon and calcium isotope ratios that is the opposite of the here presented correlation. The variations in the correlation of these isotope systems were attributed to changes of the pore fluid composition induced by bacterial sulfate-reduction and methanogenesis. These considerations do not apply to the dolomites and their geochemical data shown here (Fig. 3). In the case settings presented here, bacterial sulfate-reduction seems to be the only factor driving the isotope fractionation pattern. This assumption is supported by patterns in Mg isotope variation, relative to that of carbon and calcium. These show the opposite trend of what is documented in Blättler et al. (2015; Fig. 3). Given that the Mg isotope ratios of lacustrine/palustrine dolomites display significant relations with both $\delta^{13}C$ and $\delta^{44/40}Ca$ values—as observed via their correlations and the PCA (Figs. 3, 5C and Table 2)—we here propose that all three systems are influenced by microbial sulfate-reduction. According to Carder et al. (2005), Mg isotopes of dolomites display a significant isotope fractionation in the presence of bacterial consortia. Thus, it seems likely that the activity of sulfate-reducing bacteria has an influence on the Mg isotope composition of dolomites. Under increased activity of sulfate-reducing bacteria (Fig. 3), the $\delta^{26}Mg$ values of dolomite shift to higher values. Since different bacteria species have their own distinct Mg isotope signatures

(Carder et al., 2005), sulfate-reducing bacteria preferentially incorporate the light Mg isotope (^{24}Mg) and consequently, the dolomite is enriched in the heavier Mg isotope (^{26}Mg). This concept, however, must be tested in forthcoming work. Rayleigh-type distillation would lead to a similar increase of the δ^{26}Mg values of dolomite. When the supply of Mg is limited, the δ^{26}Mg values of dolomite is expected to increase.

Summing up, δ^{13}C, $\delta^{44/40}$Ca and δ^{26}Mg of lacustrine/palustrine dolomites all are influenced (but to different degrees) by the activity of sulfate-reducing bacteria (Figs. 5C and 6). Oxygen isotope data, in contrast, are independent of the factor driving variations of the other three isotope systems as shown by PCA (Fig. 5C and Table 2), but rather reflect the groundwater source for playa and coal ball dolomites (δ^{18}O values between -8.82 to -1.30‰). In the case of the lake dolomite, with an elevated δ^{18}O value of +3.70‰, evaporation is likely to have influenced the water isotopic composition.

4.4 On the applicability of calcium isotopes in dolomite research

Data on the quaternary isotope system and cation ordering degree of the various early diagenetic dolomites shown here reveal a very high level of complexity with regard to their early diagenetic formation and subsequent alteration (Fig. 6). When comparing early diagenetic sabkha dolomites with lacustrine/palustrine ones, it becomes obvious that sabkha dolomites reflect mainly a marine source whereas lacustrine/palustrine dolomites mainly record the influence by bacterial induced sulfate-reduction. This is not intuitive, as also the lacustrine/palustrine dolomites formed during marine ingressions. In both cases, dolomite precipitation is most likely related to, or is induced by, microbial activity (Bontognali et al., 2010; Krause et al., 2012). Conversely, recrystallized sabkha and altered (meteoric overprint) marine dolomites both reflect fluid-buffered conditions. Summing up, all of the proxy data shown here respond very differently to their ambient fluids.

Generally, dolomite calcium isotope data as shown here document that this proxy is valid and has remarkable potential but is perhaps at present underexplored. Judging from published work and data shown here, $\delta^{44/40}$Ca data have a bearing on: (i) dolomite recrystallization, (ii) the degree of bacterial activity affecting the formation and stabilization of calcian dolomite (or very high-Mg calcite), (iii) the degree of buffering in a fluid- or rock-dominated system, as well as (iv) the potential to act as semi-quantitative archives for the Ca isotopic composition of the parent fluid (seawater, diagenetic fluid, groundwater) and its isotopic evolution through geological time. The full potential of the dolomite Ca isotope proxy, however, only unfolds when combined with data of the other main elements (C, O, Mg) of Mg-

carbonates. The Ca isotope proxy acts as a benchmark against which other proxy data can be calibrated or processes tested. Circumstantial evidence comes from optical (e.g., petrography based on transmitted light microscopy, cathodoluminescence) and geochemical tools (e.g., elemental concentrations, $^{87}Sr/^{86}Sr$ ratios). Interestingly, even the limited data sets shown here point to patterns that can be interpreted in a meaningful manner and are of relevance for dolomite research. Clearly, results and hypotheses presented here must be tested, verified or falsified in forthcoming work.

5. CONCLUSIONS

The interpretation of the calcium isotope proxy using dolomite is challenging but feasible when placed in the context of a multi-proxy approach and well-constrained environmental data. The application of the quaternary isotope approach comprising C, O, Mg and Ca in combination with the cation ordering degree (COD) sheds light on dolomite formation and alteration processes and products. The potential to reconstruct the Ca isotopic composition of the environmental or diagenetic fluid, from which the dolomite precipitated, is considered critically. Care must be taken, however, as early marine diagenetic dolomites represent metastable archives and they subsequently stabilize in the presence of pore fluids that might differ, to some degree, from open marine seawater or lacustrine/palustrine waters.

Our data document that in the case of sabkha dolomites COD, C and Ca isotope ratios are influenced by kinetic and equilibrium isotope fractionation (primary and recrystallized dolomite, respectively). In contrast, Mg isotope values of sabkha dolomites are affected by microbial activity. The calculated $\Delta^{44/40}Ca_{dolomite\text{-}fluid}$ for primary sabkha dolomites ranges between -0.4 and -1.3‰. Arguments are brought forward to place $\Delta^{44/40}Ca_{dolomite\text{-}fluid}$ at (or near) 0‰ for recrystallized dolomites and hence, their $\delta^{44/40}Ca_{dolomite}$ value reflects, within limitations, the seawater or marine pore fluid Ca isotope signature from which it is formed. This implies that relative trends in seawater/pore fluid $\delta^{44/40}Ca$ signature throughout geological time can be assessed from these data. Statements regarding absolute seawater values must be treated with care.

Isotope signatures of altered marine dolomites are separated into two clusters: Carbon isotope values still represent the initial marine source, whereas $\delta^{18}O$, $\delta^{26}Mg$ and $\delta^{44/40}Ca$ reflect a meteoric diagenetic fluid source. In the case of the samples studied here, isotopic signatures of Mg and Ca and the lack of correlation with $\delta^{13}C$ suggest a silicate bedrock aquifer in contact with the meteoric fluid.

Lacustrine/palustrine dolomites, formed during marine ingressions, display correlations between C, Mg and Ca isotope values, but none with O. These dolomites precipitated under intense microbial influence, particularly sulfate reducers. The metabolic activity of these bacteria leads to enhanced fractionation of C, Mg and Ca isotope composition compared to playa and lake environments.

The combination of the four isotope proxies and the COD clearly improves our potential to reconstruct environmental signals and processes during diagenetic pathways. Having said this, the multi-proxy data set shown here and the level of complexity found in different dolomite formation and alteration environments—as revealed by these data—represent a clear warning against sophisticated interpretations of proxy data from unspecified bulk data sets.

Acknowledgments

This is a contribution of the collaborative research initiative CHARON (DFG Forschergruppe 1644) funded by the German and Austrian Science Foundations (Grants: IM44/10-2, DI796/2-2 and FWF-I3028-N29). A. Geske is thanked for providing dolomite samples. We thank T. Reinecke for numerous XRD analyses. The support of B. Gehnen and K. Krimmler at the isotope laboratory at Bochum is greatly acknowledged. We thank the associate editor A. Turchyn and three anonymous reviewers for their exceptionally constructive input on our manuscript.

References

Ahm A.-S. C., Bjerrum C. J., Blättler C. L., Swart P. K. and Higgins J. A. (2018) Quantifying early marine diagenesis in shallow-water carbonate sediments. *Geochimica et Cosmochimica Acta* **236**, 140-159.

Ahm A.-S. C., Maloof A. C., Macdonald F. A., Hoffmann P. F., Bjerrum C. J., Bold U., Rose C. V., Strauss J. V. and Higgins J. A. (2019) An early diagenetic deglacial origin for basal Ediacaran "cap dolostones". *Earth and Planetary Science Letters* **506**, 292-307.

AlKhatib M. and Eisenhauer A. (2017) Calcium and strontium isotope fractionation in aqueous solutions as a function of temperature and reaction rate; I. Calcite. *Geochimica et Cosmochimica Acta* **209**, 296-319.

Baker P. A. and Kastner M. (1981) Constraints on the formation of sedimentary dolomite. *Science* **213**, 214-216.

729 Blättler C. L., Miller N. R. and Higgins J. A. (2015) Mg and Ca isotope signatures of authigenic
730 dolomite in siliceous deep-sea sediments. *Earth and Planetary Science Letters* **419**, 32-
731 42.
732 Bontognali T. R. R., Vasconcelos C., Warthmann R. J., Bernasconi S. M., Dupraz C.,
733 Strohmenger C. J. and McKenzie J. A. (2010) Dolomite formation within microbial
734 mats in the coastal sabkha of Abu Dhabi (United Arab Emirates). *Sedimentology* **57**,
735 824-844
736 Bradbury H. J. and Turchyn A. V. (2018) Calcium isotope fractionation in sedimentary pore
737 fluids from ODP Leg 175: Resolving carbonate recrystallization. *Geochimica et*
738 *Cosmochimica Acta* **236**, 121-139.
739 Bradbury H. J., Halloran K. H., Lin C. Y. and Turchyn A. V. (2020) Calcium isotope
740 fractionation during microbially induced carbonate mineral precipitation. *Geochimica*
741 *et Cosmochimica Acta* **277**, 37-51.
742 Bradley W. F., Burst J. F. and Graf D. L. (1953) Crystal chemistry and differential thermal
743 effects of dolomite. *American Mineralogist* **38**, 207-217.
744 Budd D. A. (1997) Cenozoic dolomites of carbonate islands: their attributes and origin. *Earth*
745 *Science Reviews* **42**, 1-47.
746 Carder E. A., Galy A., McKenzie J. A., Vasconcelos C. and Elderfield H. E. (2005) Magnesium
747 isotopes in bacterial dolomites: A novel approach to the dolomite problem,
748 Goldschmidt, Moscow, Idaho, USA, p. A213.
749 Chai L., Navrotsky A. and Reeder R. J. (1995) Energetics of calcium-rich dolomite.
750 *Geochimica et Cosmochimica Acta* **59 (5)**, 939-944.
751 Claypool G. E. and Kaplan I. R. (1974) The origin and distribution of methane in marine
752 sediments. In *Natural gases in marine sediments* (eds. I. R. Kaplan). Springer US, New
753 York. pp. 99-139.
754 Fantle M. S. and DePaolo D. J. (2007) Ca isotopes in carbonate sediment and pore fluid from
755 ODP Site 807A: The Ca^{2+} (aq)-calcite equilibrium fractionation factor and calcite
756 recrystallization rates in Pleistocene sediments. *Geochimica et Cosmochimica Acta* **71**,
757 2524-2546.
758 Fantle M. S. and Higgins J. (2014) The effects of diagenesis and dolomitization on Ca and Mg
759 isotopes in marine platform carbonates: Implications for the geochemical cycles of Ca
760 and Mg. *Geochimica et Cosmochimica Acta* **142**, 458-481.
761 Farkaš J., Böhm F., Wallmann K., Blenkinsop J., Eisenhauer A., van Geldern R.,

762 Munnecke A., Voigt S. and Veizer J. (2007) Calcium isotope record of Phanerozoic
763 oceans: implications for chemical evolution of seawater and its causative mechanisms.
764 *Geochimica et Cosmochimica Acta* **71**, 5117-5134.
765 Geske A., Goldstein R. H., Mavromatis V., Richter D. K., Buhl D., Kluge T., John C. M. and
766 Immenhauser A. (2015a) The magnesium isotope (δ^{26}Mg) signature of dolomites.
767 *Geochimica et Cosmochimica Acta* **149**, 131-151.
768 Geske A., Lokier S., Dietzel M., Richter D. K., Buhl D. and Immenhauser A. (2015b)
769 Magnesium isotope composition of sabkha pore fluid and related (Sub-) Recent
770 stoichiometric dolomites, Abu Dhabi (UAE). *Chemical Geology* **393-394**, 112-124.
771 Geske A., Zorlu J., Richter D. K., Buhl D., Niedermayr A. and Immenhauser A. (2012)
772 Impact of diagenesis and low grade-metamorphosis on isotope (δ^{26}Mg, δ^{13}C, δ^{18}O and
773 ^{87}Sr/^{86}Sr) and elemental (Ca, Mg, Mn, Fe and Sr) signatures of Triassic sabkha
774 dolomites. *Chemical Geology* **332-333**, 45-64.
775 Gregg J. M., Bish D. L., Kaczmarek S. E. and Machel H. G. (2015) Mineralogy, nucleation and
776 growth of dolomite in the laboratory and sedimentary environment: A review.
777 *Sedimentology* **62**, 1749-1769.
778 Gussone N. and Dietzel M. (2016) Calcium isotope fractionation during mineral precipitation
779 from aqueous solution. In *Calcium stable isotope geochemistry* (eds. N. Gussone, A.-
780 D. Schmitt, A. Heuser, F. Wombacher, M. Dietzel, E. T. Tipper and M. Schiller).
781 Springer, Berlin. pp. 75-144.
782 Gussone N., Böhm F., Eisenhauer A., Dietzel M., Heuser A., Teichert B. M. A., Reitner J.,
783 Wörheide G. and Dullo W.-C. (2005) Calcium isotope fractionation in calcite and
784 aragonite. *Geochimica et Cosmochimica Acta* **69**, 4485-4494.
785 Hammer O., Harper D. A. T. and Ryan P. D. (2001) PAST: Paleontological statistics software
786 package for education and data analysis. *Palaeontologia Electronica* **4(1)**, 9pp.
787 Heuser A., Schmitt A.-D., Gussone N. and Wombacher F. (2016) Analytical Methods. In
788 *Calcium stable isotope geochemistry* (eds. N. Gussone, A.-D. Schmitt, A. Heuser, F.
789 Wombacher, M. Dietzel, E. T. Tipper and M. Schiller). Springer, Berlin. pp. 23-73.
790 Higgins J. A., Blättler C. L., Lundstrom E. A., Santiago-Ramos D. P., Akhtar A. A., Crüger
791 Ahm A.-S., Bialik O., Holmden C., Bradbury H., Murray S. T. and Swart P. K. (2018)
792 Mineralogy, early marine diagenesis, and the chemistry of shallow-water carbonate
793 sediments. *Geochimica et Cosmochimica Acta* **220**, 512-534.
794 Hippler D., Witbaard R., van Aken H. M., Buhl D. and Immenhauser A. (2013) Exploring the

795 calcium isotope signature of Arctica islandica as an environmental proxy using
796 laboratory- and field-cultured specimens. *Paleogeogr. Paleoclimatol. Paleoecol.* **373**,
797 75-87.
798 Holmden C. (2009) Ca isotope study of Ordovician dolomite, limestone, and anhydrite in the
799 Williston Basin: Implications for subsurface dolomitization and local Ca cycling.
800 *Chemical Geology* **268**, 180-188.
801 Holmden C., Papanastassiou D. A., Blanchon P. and Evans S. (2012) $\delta^{44/40}$Ca variability in
802 shallow water carbonates and the impact of submarine groundwater discharge on Ca-
803 cycling in marine environments. *Geochimica et Cosmochimica Acta* **83**, 179-194.
804 Jacobson A. D. and Holmden C. (2008) δ^{44}Ca evolution in a carbonate aquifer and its bearing
805 on the equilibrium isotope fractionation factor for calcite. *Earth and Planetary Science*
806 *Letters* **270**, 349-353.
807 Jones D. S., Brothers R. W., Ahm A.-S. C., Slater N., Higgins J. A. and Fike D. A. (2020) Sea
808 level, carbonate mineralogy, and early diagenesis controlled δ^{13}C records in Upper
809 Ordovician carbonates. *Geology* **48**, 194-199.
810 Kasemann S. A., Hawkesworth C. J., Prave A. R., Fallick A. E. and Pearson P. N. (2005) Boron
811 and calcium isotope composition in Neoproterozoic carbonate rocks from Namibia:
812 evidence for extreme environmental change. *Earth and Planetary Science Letters* **231**,
813 73-86.
814 Kasemann S. A., Pogge von Strandmann P. A. E., Prave A. R., Fallick A. E., Elliott T. and
815 Hoffmann K.H. (2014) Continental weathering following a Cryogenian glaciation:
816 Evidence from calcium and magnesium isotopes. *Earth and Planetary Science Letters*
817 **396**, 66-77.
818 Kell-Duivestein I. J., Baldermann A., Mavromatis V. and Dietzel M. (2019) Controls of
819 temperature, alkalinity and calcium carbonate reactant on the evolution of dolomite and
820 magnesite stoichiometry and dolomite cation ordering degree - An experimental
821 approach. *Chemical Geology* **529**, 119292.
822 Kelts K. R. and McKenzie J. A. (1982) Diagenetic dolomite formation in Quaternary anoxic
823 diatomaceous muds of Deep Sea Drilling Project Leg 64, Gulf of California. *Initial*
824 *Report Deep Sea Drilling Project* **64 (2)**, 553-569.
825 Komiya T., Suga A., Ohn, T., Han J., Guo J., Yamamoto S., Hirata T. and Li Y. (2008) Ca
826 isotopic compositions of dolomite, phosphorite and the oldest animal embyo fossils
827 from the Neoproterozoic in Weng'an, South China. *Gondwana Research* **14**, 209-218.
828 Krause S., Liebetrau V., Gorb S., Sánchez-Román M., McKenzie J.A. and Treude T. (2012)

Microbial nucleation of Mg-rich dolomite in exopolymeric substances under anoxic modern seawater salinity: New insight into an old enigma. *Geology* **40**, 587-590.

Land L. S. (1973) Holocene meteoric dolomitization of Pleistocene limestones, North Jamaica. *Sedimentology* **20**, 411-424.

Land L. S. (1980) The isotopic and trace element geochemistry of dolomite: the state of the art. *SEPM Special Publication* **28**, 87-110.

Land L. S. (1982) Dolomitization. American Association of Petroleum Geologists, Tulsa.

Land L. S. (1985) The origin of massive dolomite. *Journal of Geoscience Education* **33**, 112-125.

Land L. S. (1998) Failure to precipitate dolomite at 25 degrees C from dilute solution despite 1000-fold oversaturation after 32 years. *Aquatic Geochemistry* **4 (3-4)**, 361-368.

Lemarchand D., Wasserburg G. J. and Papanastassiou D. A. (2004) Rate-controlled calcium isotope fractionation in synthetic calcite. *Geochimica et Cosmochimica Acta* **68**, 4665-4678.

Lokier S., Knaf A. and Kimiagar S. (2013) A quantitative analysis of recent arid coastal sedimentary facies from the Arabian Gulf Coastline of Abu Dhabi, United Arab Emirates. *Marine Geology* **346**, 141-152.

Lowenstam H. and Epstein S. (1957) On the origin of sedimentary aragonite needles of Great Bahama Bank. *Journal of Geology* **65**, 364-375.

Machel H. G. (2004) Concepts and models of doloitization: A critical reappraisal. In: *The Geometry and Petrogenesis of Dolomite Hydrocarbon Reservoirs* (eds. C. J. R. Braithwaite, G. Rizzi and G. Darke). Geological Society. Special Publication, London. Pp. 7-63.

Machel H. G. and Anderson J. H. (1989) Pervasive subsurface dolomitization in the Nisku formation in Central Alberta. *Journal of Sedimentary Petrology* **59**, 891-911.

Machel H. G., Krouse H. R. and Sassen R. (1995) Products and distinguishing criteria of bacterial and thermodynamical sulfate reduction. *Applied Geochemistry* **10**, 373-389.

Malone M. J., Baker P. A. and Burns S. J. (1996) Hydrothermal dolomitization and recrystallization of dolomite breccias from the Miocene Monterey Formation, Tepusquet Area, California. *J. Sediment. Res.* **66**, 976-990.

Marriott C. S., Henderson G. M. and Belshaw N. S. (2004) Temperature dependence of δ^{7}Li, δ^{44}Ca and Li/Ca during growth of calcium carbonate. *Earth and Planetary Science Letters* **222**, 615-624.

Mavromatis V., Pearce C. R., Shirokova L. S., Bundeleva I. A., Pokrovsky O. S., Benezeth P.

and Oelkers E. H. (2012) Magnesium isotope fractionation during hydrous magnesium carbonate precipitation with and without cyanobacteria. *Geochimica et Cosmochimica Acta* **76**, 161-174.

Mazzullo S. J., Bischoff W. D. and Teal C. S. (1995) Holocene shallow-subtidal dolomitization by near-normal seawater, northern Belize. *Geology* **23**, 341-344.

McKenzie J. A. (1981) Holocene dolomitization of calcium carbonate sediments from the coastal sabkhas of Abu Dhabi, U.A.E.: A stable isotope study. *Journal of Geology* **89**, 185-198.

Meyers W. J., Lu F. H. and Zachariah J. K. (1997) Dolomitization by mixed evaporative brines and freshwater, upper Miocene carbonates, Nijar, Spain. *Journal of Sedimentary Research Section A* **67**, 898-912.

Milliman J. D. (1974) *Marine Carbonates*. Springer, Berlin, pp. 375.

Morse J. W. (2005) Formation and diagenesis of carbonate sediments. In *Sediments, Diagenesis, and Sedimentary Rocks* (F. T. Mackenzie eds). Elsevier, Amsterdam. pp. 67-86.

Mueller M., Igbokwe O. A., Walter B., Pederson C. L., Riechelmann S., Richter D. K., Albert R., Gerdes A., Buhl D., Neuser R. D., Bertotti G. and Immenhauser A. (2020) Testing the preservation potential of early diagenetic dolomites as geochemical archives. *Sedimentology* **67**, 849-881.

Navarra A. and Simoncini V. (2010) *A Data Analysis Guide to Empirical Orthogonal Functions for Climate*. Springer, Dordrecht, Heidelberg, London, New York, pp. 151.

Nichols G. (2009) *Sedimentology and Stratigraphy, 2nd ed.* Wiley-Blackwell, Chichester.

Orem W. H. and Finkelman R.B. (2005) Coal formation and geochemistry. In *Sediments, Diagenesis, and Sedimentary Rocks* (F. T. Mackenzie eds). Elsevier, Amsterdam. pp. 191-222.

Owen R. A., Day C. C., Hu C. Y., Liu Y. H., Pointing M. D., Blättler C.L. and Henderson G.M. (2016) Calcium isotopes in caves as a proxy for aridity: Modern calibration and application to the 8.2 kyr event. *Earth and Planetary Science Letters* **443**, 129-138.

Perez-Fernandez A., Berninger U. N., Mavromatis V., Pogge von Strandmann P. A. E. and Oelkers E.H. (2017) Ca and Mg isotope fractionation during the stoichiometric dissolution of dolomite at temperatures from 51 to 126°C and 5bars CO_2 pressure. *Chemical Geology* **467**, 76-88.

Petrash D. A., Bialik O. M., Bontognali T. R. R., Vasconcelos C., Roberts J. A., McKenzie

J. A. and Konhauser K. O. (2017) Microbially catalyzed dolomite formation: From near-surface to burial. *Earth - Science Reviews* **171**, 558-582.

Pokrovsky B. G., Mavromatis V. and Pokrovsky O. S. (2011) Co-variation of Mg and C isotopes in late Precambrian carbonates of the Siberian Platform: A new tool for tracing the change in weathering regime? *Chemical Geology* **290**, 67-74.

Reeder R. J. (1981) Electron optical investigation of sedimentary dolomite. *Contributions to Mineralogy and Petrology* **76**, 148-157.

Reeder R. J. (1992) Carbonates: growth and alteration microstructures In *Minerals and Reactions at the Atomic Scale: Transmission Electron Microscopy* (eds. P. R. Buseck). Mineral. Soc. Am. Rev. Mineral. 27, pp. 381-424.

Richter D. K., Heinrich F., Geske A., Neuser R. D., Gies H. and Immenhauser A. (2014) First description of Phanerozoic radiaxial fibrous dolomite. *Sedimentary Geology* **304**, 1-10.

Riechelmann S., Mavromatis V., Buhl D., Dietzel M., Eisenhauer A. and Immenhauser A. (2016) Impact of diagenetic alteration on brachiopod shell magnesium isotope (δ^{26}Mg) signatures: Experimental versus field data. *Chemical Geology* **440**, 191-206.

Riechelmann S., Mavromatis V., Buhl D., Dietzel M., Hoffmann R., Jöns N., Kell-Duivestein I. and Immenhauser A. (2018) Echinoid skeletal carbonate as archive of past seawater magnesium isotope signatures – Potential and limitations. *Geochimica et Cosmochimica Acta* **235**, 333-359.

Rustad J. R., Casey W. H., Yin Q.-Z., Bylaska E. J., Felmy A. R., Bogatko S. A., Jackson V. E. and Dixon D.A. (2010) Isotopic fractionation of Mg^{2+} (aq), Ca^{2+} (aq), and Fe^{2+} (aq) with carbonate minerals. *Geochimica et Cosmochimica Acta* **74**, 6301-6323.

Ryu J.-S., Jacobsen A. D., Holmden C., Lundstrom C. and Zhang Z. (2011) The major ion, $\delta^{44/40}$Ca, $\delta^{44/42}$Ca, and $\delta^{26/24}$Mg geochemistry of granite weathering at pH=1 and T=25°C: power-law processes and the relative reactivity of minerals. *Geochimica et Cosmochimica Acta* **75**, 6004-6026.

Silva-Tamayo J. C., Nägler, T. F., Sial A. N., Nogueira A., Kyser K., Riccomini C., James N. P., Narbonne G. M. and Villa I. M. (2010) Global perturbation of the marine Ca isotopic composition in the aftermath of the Marinoan global glaciation. *Precambrian Research* **182**, 373-381.

Sime N. G., De La Rocha C. L. and Galy A. (2005) Negligible temperature dependence of calcium isotope fractionation in 12 species of planktonic foraminifera. *Earth and Planetary Science Letters* **232**, 51-66.

Stanley S. M. and Hardie L. A. (1998) Secular oscillations in the carbonate mineralogy of

reef-building and sediment-producing organisms driven by tectonically forced shifts in seawater chemistry. *Palaeogeography, Palaeoclimatology, Palaeoecology* **144**, 3-19.

Steuber T. and Buhl D. (2006) Calcium isotope fractionation in selected modern and ancient marine carbonates. *Geochimica et Cosmochimica Acta* **70**, 5507-5521.

Swart P. K., Cantrell D. L., Westphal H., Handford R. and Kendall C. G. (2005) Origin of dolomite in the Arab-D reservoir from the Ghawar field, Saudi Arabia: Evidence from petrographic and geochemical constraints. *Journal of Sedimentary Research* **75**, 476-791.

Tang J., Dietzel M., Böhm F., Köhler S.J. and Eisenhauer A. (2008) Sr^{2+}/Ca^{2+} and $^{44}Ca/^{40}Ca$ fractionation during inorganic calcite formation: II. Ca isotopes. *Geochimica et Cosmochimica Acta* **72**, 3733-3745.

Teng F. Z. (2017) Magnesium Isotope Geochemistry. In *Non-Traditional Stable Isotopes* (F. Z. Teng, J. Watkins and N. Dauphas eds). Mineralogical Soc Amer & Geochemical Soc, Chantilly. pp. 219-287.

Tipper E. T., Galy A. and Bickle M. J. (2008) Calcium and magnesium isotope systematics in rivers draining the Himalaya-Tibetan-Plateau region: Lithological or fractionation control? *Geochimica et Cosmochimica Acta* **72**, 1057-1075.

Tipper E. T., Schmitt A.-D. and Gussone N. (2016) Global Ca cycles: Coupling of continental and oceanic processes. In *Calcium stable isotope geochemistry* (eds. N. Gussone, A.-D. Schmitt, A. Heuser, F. Wombacher, M. Dietzel, E. T. Tipper and M. Schiller). Springer, Berlin. pp. 173-222.

Vahrenkamp V.C. and Swart P. K. (1990) New distribution coefficient for the incorporation of strontium into dolomite and its implication for the formation of ancient dolomites. *Geology* **18**, 387–391.

Vasconcelos C., McKenzie J. A., Bernasconi S., Grujic D. and Tien A. J. (1995) Microbial mediation as a possible mechanism for natural dolomite formation at low temperatures. *Nature* **377**, 220-222.

Von der Borch C. C., Lock D. and Schwebel D. (1975) Ground-water formation of dolomite in the Coorong region of South Australia. *Geology* **3**, 283-285.

von Storch H. and Zwiers F. W. (2002) *Statistical Analysis in Climate Research*. Cambridge University Press, Cambridge, pp. 293.

Walter, B.F., Immenhauser, A., Geske, A., and Markl, G. (2015) Exploration of hydrothermal carbonate magnesium isotope signatures as tracers for continental fluid aquifers, Schwarzwald mining district, SW Germany. *Chemical Geology* **400**, 87-105.

964 Wang S., Yan W., Magalhães V. H., Chen Z., Pinheiro L. M. and Gussone N. (2012) Calcium
965 isotope fractionation and its controlling factors over authigenic carbonates in the cold
966 seeps of the northern South China Sea. *Chinese Science Bulletin* **57**, 1325-1332.
967 Wang S., Yan W., Magalhães V. H., Chen Z., Pinheiro L. M. and Gussone N. (2014) Factors
968 influencing methane-derived authigenic carbonate formation at cold seep from
969 southwestern Dongsha area in the northern South China Sea. Environ. *Earth Sci.* **71**, 20-
970 87-2094.
971 Wang W., Qin T., Zhou C., Huang S., Wu Z. and Huang F. (2017) Concentration effect on
972 equilibrium fractionation of Mg-Ca isotopes in carbonate minerals: Insights from first-
973 principles calculations. *Geochimica et Cosmochimica Acta* **208**, 185-197.
974 Warren J. (2000) Dolomite: occurence, evolution and economically important associations.
975 *Earth-Science Reviews* **52**, 1-81.
976 Wieser M. E., Buhl D., Bouman C. and Schwieters J. (2004) High precision calcium isotope
977 ratio measurements using a magnetic sector multiple collector inductively coupled
978 plasma mass spectrometer. *Journal of Analytical Atomic Spectrometry* **19**, 844-851.
979 Wombacher F., Eisenhauer A., Heuser A. and Weyer S. (2009) Separation of Mg, Ca and Fe
980 from geological reference materials for stable isotope ratio analyses by MC-ICP-MS
981 and double-spike TIMS. *Journal of Analytical Atomic Spectrometry* **24**, 627-636.
982 Zhang F., Xu H., Konishi H., Shelobolina E. S. and Roden E. E. (2012) Polysaccharide-
983 catalyzed nucleation and growth of disordered dolomite: A potential precursor of
984 sedimentary dolomite. *American Mineralogist* **97**, 556-567.
985 Zhou Y. L., Wang S. J., Hilton J., Tian B. L. (2008) Anatomically preserved lepidodendralean
986 plants from Lower Permian coal balls of northern China: *Achlamydocarpon*
987 *intermedium* sp. nov. *Plants Systematics and Evolution* **273**, 71-85.
988
989
990
991
992
993
994
995
996

997 Table 1. Chemical composition of the herein studied distinct dolomite types, where data on
998 cation ordering degree of dolomite (COD), $\delta^{26}Mg$, $\delta^{13}C$, and $\delta^{18}O$ are from Geske et al. (2015a).
999 $\delta^{44/42}Ca$ (‰ IAPSO) are converted to $\delta^{44/40}Ca$ (‰ SRM 915a) values using the equations given
1000 by Heuser et al. (2016).

No.	Sample	COD	$\delta^{26}Mg$ (‰ DSM3)	±2σ	$\delta^{13}C$ (‰ VPDB)	±σ	$\delta^{18}O$ (‰ VPDB)	±σ	$\delta^{44/42}Ca$ (‰ IAPSO)	±2σ	$\delta^{44/40}Ca$ (‰ SRM 915a)	±2σ
Sabkha dolomite												
1	2a10	0.36	-2.49	0.08	3.77	0.03	-2.16	0.03	-0.66	0.03	0.53	0.06
2	2a12	0.21	-2.44	0.06	3.90	0.03	-1.72	0.04	-0.57	0.01	0.72	0.03
3	HDK51	0.66	-1.99	0.07	2.59	0.03	-1.38	0.05	-0.55	0.04	0.75	0.08
4	1b23	0.53	-2.24	0.10	4.83	0.03	-1.10	0.05	-0.55	0.06	0.76	0.13
5	Bel1a	0.53	-2.20	0.06	0.58	0.02	-3.39	0.02	-0.50	0.08	0.86	0.16
7	Oo	0.43	-1.70	0.03	7.20	0.04	1.48	0.03	-0.74	0.07	0.37	0.13
8	Oom	0.43	-1.71	0.02	7.11	0.02	1.83	0.01	-0.74	0.06	0.36	0.12
9	Kri	0.65	-2.03	0.06	4.41	0.02	-0.81	0.02	-0.67	0.05	0.50	0.10
10	Angola 1	0.93	-1.67	0.05	1.34	0.02	-12.37	0.02	-0.34	0.06	1.19	0.12
11	B30	0.72	-2.05	0.02	0.70	0.05	0.30	0.05	-0.49	0.06	0.88	0.13
12	B31a	0.48	-2.17	0.04	2.08	0.03	1.20	0.04	-0.47	0.05	0.91	0.11
13	B31b	0.50	-2.28	0.02	2.05	0.04	0.62	0.03	-0.48	0.07	0.89	0.13
14	B31c	0.56	-2.40	0.03	2.00	0.02	1.38	0.04	-0.47	0.03	0.91	0.07
Mean		0.54	-2.11	0.56	3.27	2.18	-1.24	3.71	-0.56	0.24	0.74	0.48
Altered marine dolomite												
15	Moggast1	0.93	-1.86	0.04	3.01	0.02	-3.50	0.05	-0.47	0.02	0.92	0.05
16	Hund1	0.84	-1.30	0.05	2.75	0.03	-4.62	0.03	-0.64	0.04	0.58	0.08
17	Contrin2	0.84	-1.38	0.07	3.14	0.03	-4.25	0.04	-0.50	0.04	0.85	0.09
18	Prüstr. 4	1.00	-1.10	0.05	-0.57	0.05	-4.44	0.03	-0.58	0.03	0.69	0.07
Mean		0.90	-1.41	0.64	2.08	1.78	-4.20	0.49	-0.55	0.15	0.76	0.31
Lacustrine/palustrine dolomite												
Playa dolomite												
19	Ofeu 3	0.67	-2.08	0.09	-7.60	0.03	-8.82	0.04	-0.47	0.03	0.91	0.07
Lake dolomite												
22	StBe20	0.52	-1.51	0.04	-1.43	0.03	3.70	0.04	-0.50	0.05	0.85	0.09
Coal ball dolomite (swamp)												
26	ToDol1	0.38	-1.15	0.04	-11.76	0.02	-5.36	0.02	-0.60	0.01	0.66	0.03
27	ToDol2	0.37	-0.72	0.02	-22.10	0.01	-4.03	0.02	-0.65	0.03	0.56	0.06
28	ToDol3	0.39	-0.91	0.02	-17.47	0.01	-1.30	0.04	-0.65	0.02	0.55	0.05
30	ToDol5	0.38	-1.13	0.05	-13.94	0.01	-5.99	0.02	-0.55	0.06	0.74	0.13
31	ToDol6	0.38	-0.53	0.02	-20.69	0.02	-4.43	0.03	-0.59	0.03	0.67	0.05
32	ToDol8	0.36	-1.07	0.04	-13.75	0.02	-5.74	0.03	-0.63	0.04	0.59	0.09
Mean		0.43	-1.14	0.96	-13.59	6.82	-4.00	3.76	-0.58	0.13	0.69	0.27

1001 Table 2. Results of the Principal Component Analysis (PCA). PC 1 to PC 5 represent the
1002 principal components or factors influencing the variations of the different proxies. The value
1003 given for % variance displays how much of the variability of the proxies can be explained by
1004 one component or factor. The remaining values are the loadings, which are the linear
1005 combination coefficients.

	PC 1	PC 2	PC 3	PC 4	PC 5
Sabkha dolomite					
% variance	54	30	10	3	2
COD	0.49	0.37	0.40	-0.60	0.33
$\delta^{26}Mg$	0.06	0.78	0.21	0.49	-0.33
$\delta^{13}C$	-0.50	0.39	-0.27	0.05	0.72
$\delta^{18}O$	-0.46	-0.22	0.85	0.12	0.11
$\delta^{44/40}Ca$	0.55	-0.24	0.08	0.62	0.50
Altered marine dolomite					
% variance	61	34	5		
COD	-0.12	0.74	-0.22		
$\delta^{26}Mg$	-0.55	-0.04	0.54		
$\delta^{13}C$	0.41	-0.53	-0.08		
$\delta^{18}O$	0.52	0.32	-0.17		
$\delta^{44/40}Ca$	0.49	0.25	0.79		
Lacustrine/palustrine dolomite					
% variance	68	23	5	4	0.2
COD	0.50	-0.14	0.60	-0.43	0.43
$\delta^{26}Mg$	-0.52	0.14	0.31	0.44	0.65
$\delta^{13}C$	0.48	0.33	-0.61	0.11	0.52
$\delta^{18}O$	0.00	0.92	0.28	-0.14	-0.23
$\delta^{44/40}Ca$	0.50	-0.04	0.30	0.77	-0.25

1006

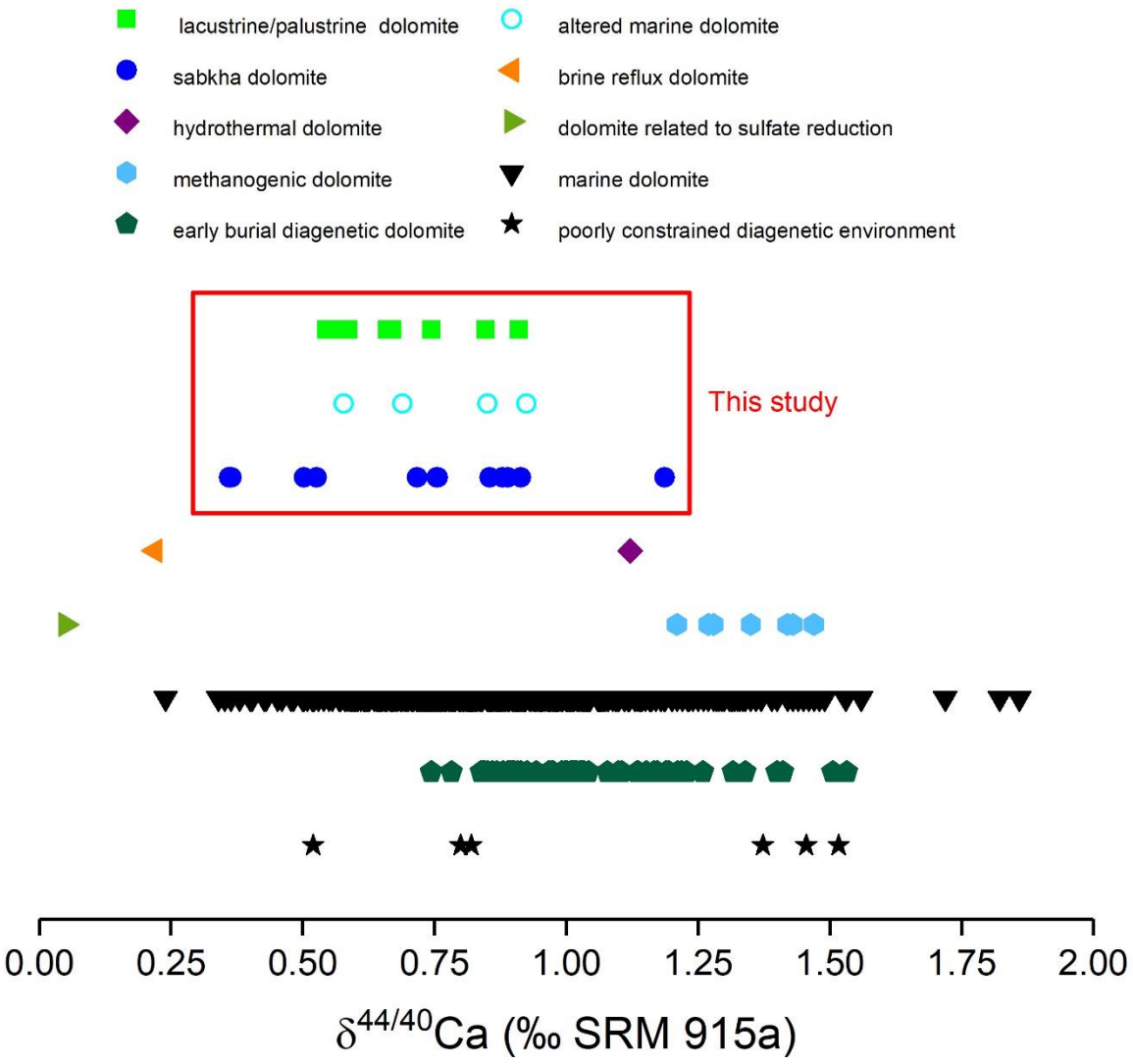

Figure 1: The Ca isotopic composition of pure dolomite samples in context of their formation environment based on literature data and this study. Lacustrine/palustrine dolomite, altered marine dolomite and sabkha dolomites are from this study. Calcium isotope data on: (i) marine dolomite are from Kasemann et al. (2005; 2014), Jacobson and Holmden (2008), Komiya et al. (2008), Silva-Tamayo et al. (2010), Fantle and Higgins (2014), Higgins et al. (2018), Ahm et al. (2018; 2019), and Jones et al. (2020). (ii) Hydrothermal dolomite is from Steuber and Buhl (2006). (iii) Early burial diagenetic dolomite is from Blättler et al. (2015). (iv) Calculated endmember for brine reflux dolomite is from Holmden (2009). (v) Experimentally dolomite related to sulfate-reduction is from Krause et al. (2012). (vi) Methanogenetic dolomite is from Wang et al. (2012; 2014). (vii) Dolomite from poorly constrained diagenetic environments are from Tipper et al. (2008), Wombacher et al. (2009) and Owen et al. (2016).

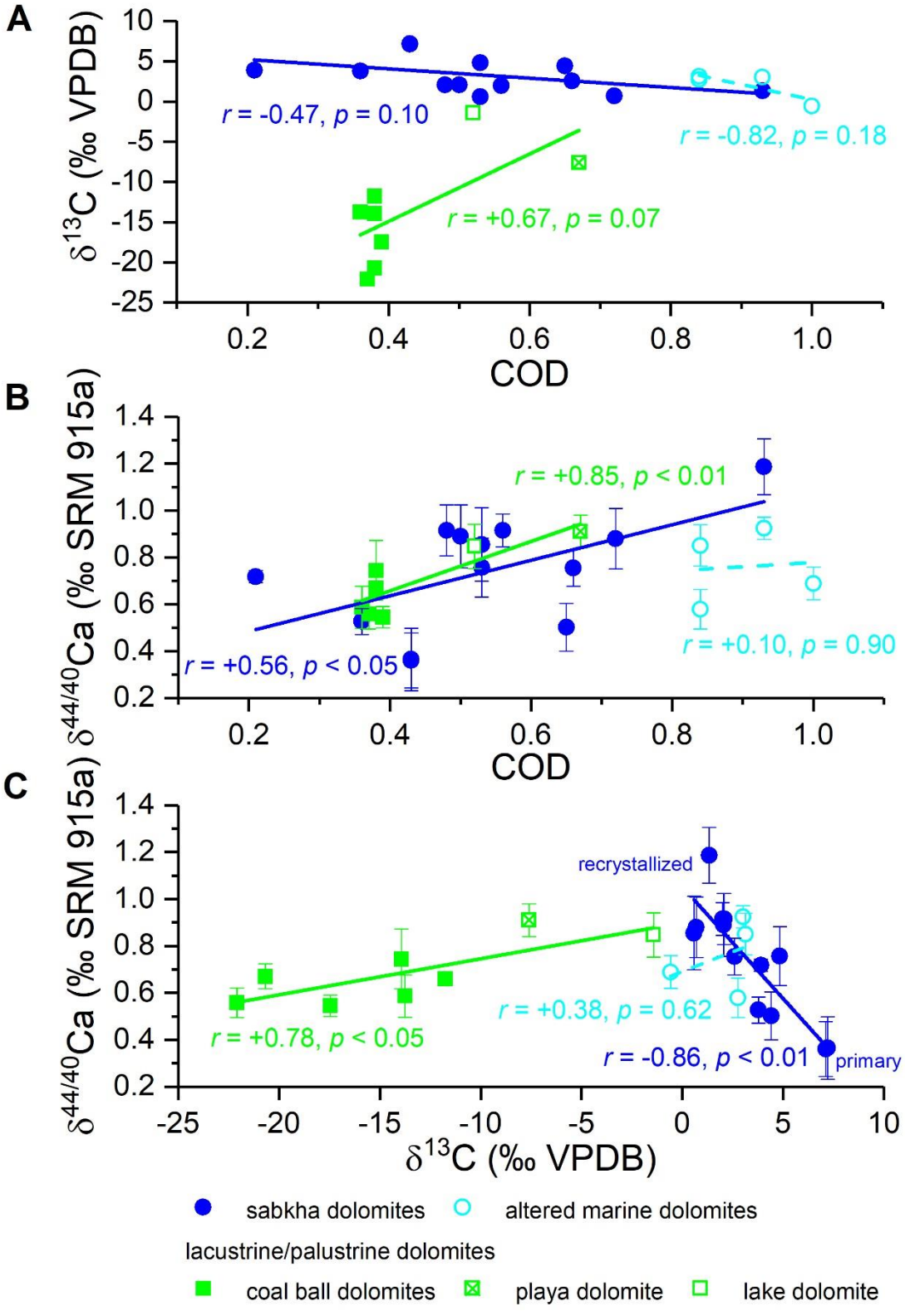

Figure 2: (A) Cation ordering degree (COD) and $\delta^{13}C$ values. **(B)** COD and $\delta^{44/40}Ca$ values, and **(C)** $\delta^{13}C$ and $\delta^{44/40}Ca$ values of sabkha, altered marine and lacustrine/palustrine dolomites (coal ball, playa and lake dolomite). Dolomites with a low COD are marked as primary dolomites, whereas dolomites with a high COD are indicated as recrystallized dolomites such as in the case of sabkha dolomites. Correlations (*r*) and their significance (*p*) are given.

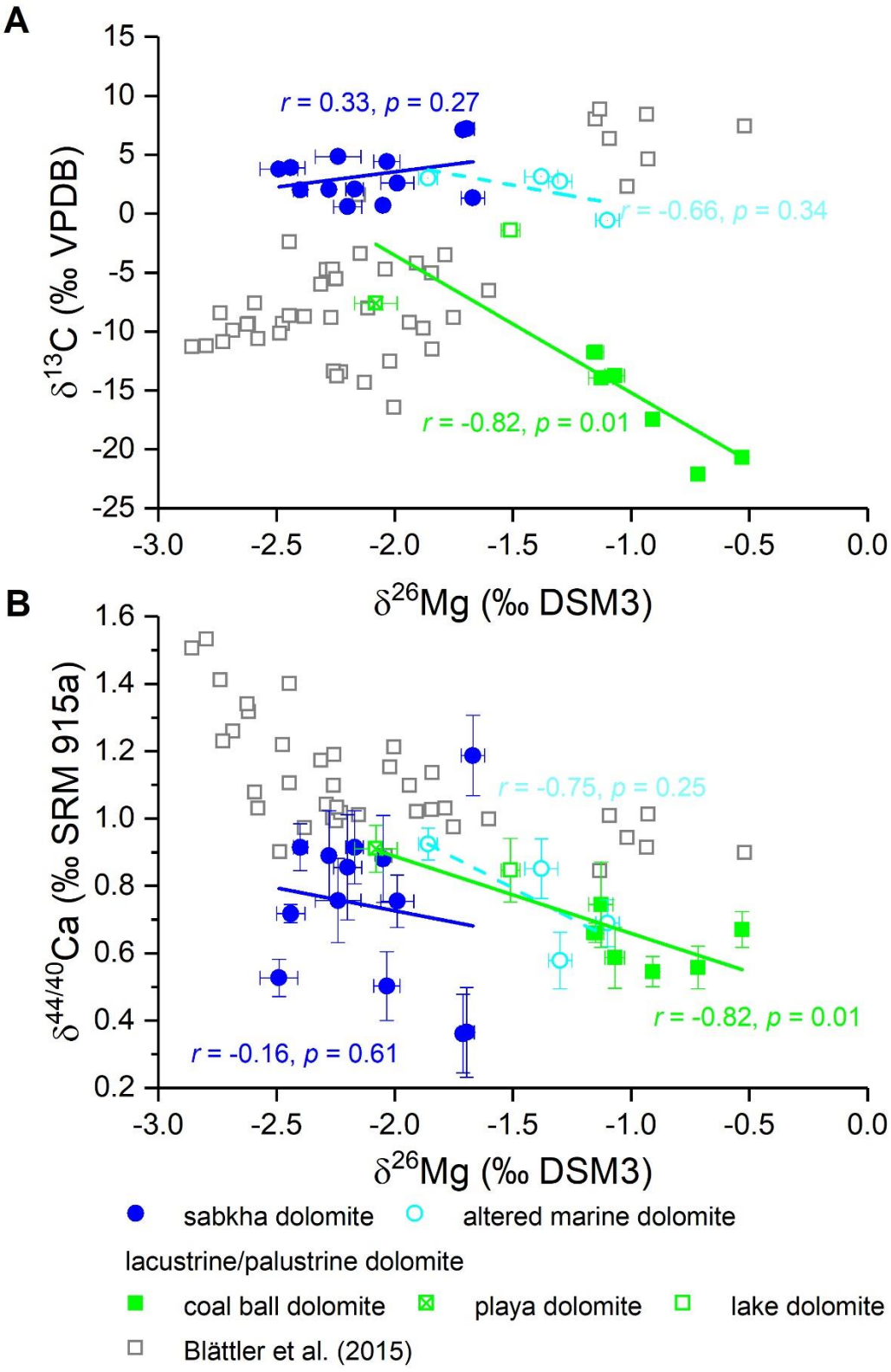

Figure 3: (A) δ^{26}Mg and δ^{13}Cvalues, and **(B)** δ^{26}Mg and $\delta^{44/40}$Ca values of sabkha, altered marine and lacustrine/palustrine dolomites (coal ball, playa, and lake dolomite). For comparison, data from Blättler et al. (2015) are plotted. Correlations (*r*) and their significance (*p*) between the proxies are given.

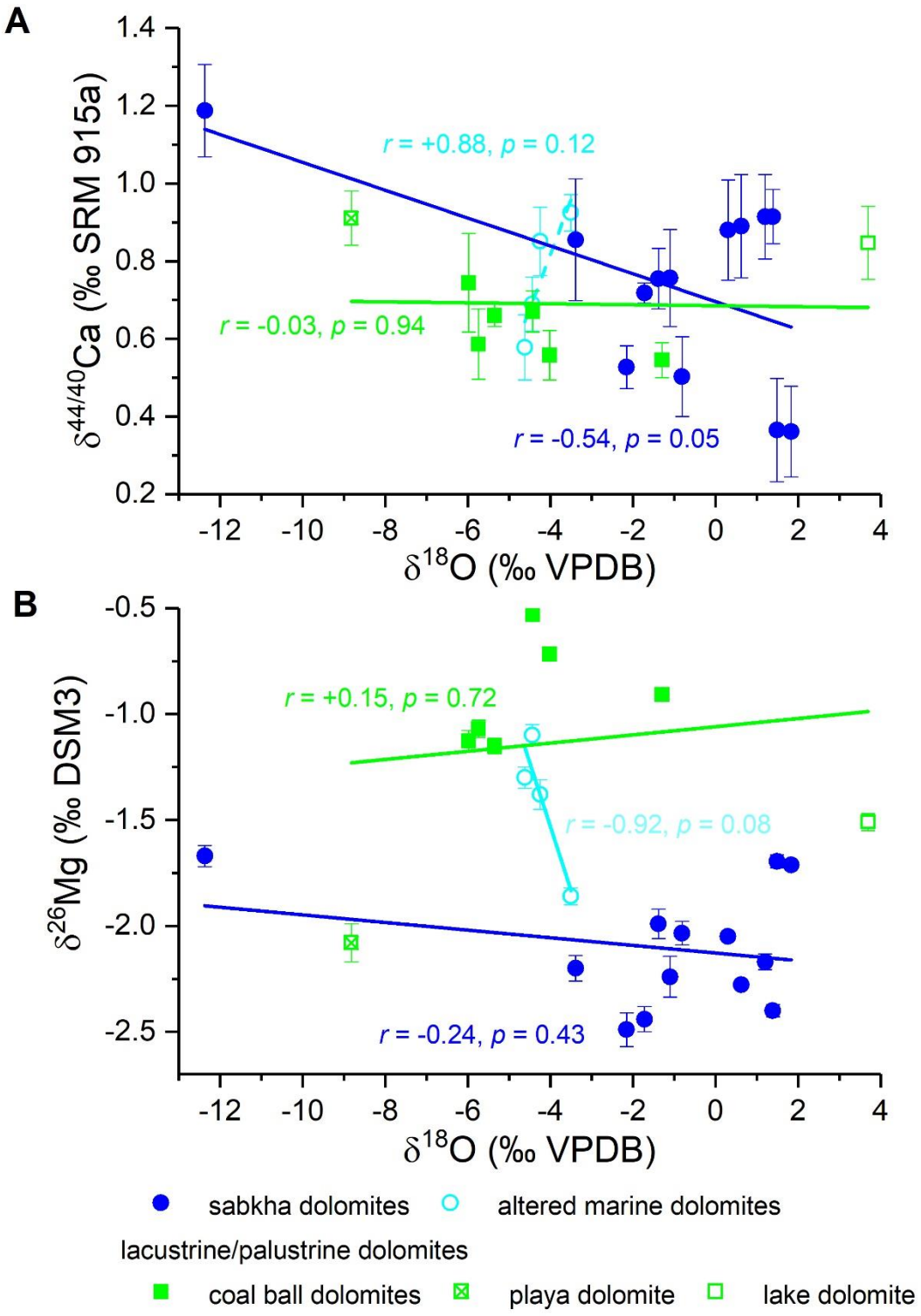

Figure 4: (A) $\delta^{18}O$ and $\delta^{44/40}Ca$ values, and **(B)** $\delta^{18}O$ and $\delta^{26}Mg$ values of sabkha, altered marine and lacustrine/palustrine dolomites (coal ball, playa, and lake dolomite). Correlations (*r*) and their significance (*p*) between the proxies are given.

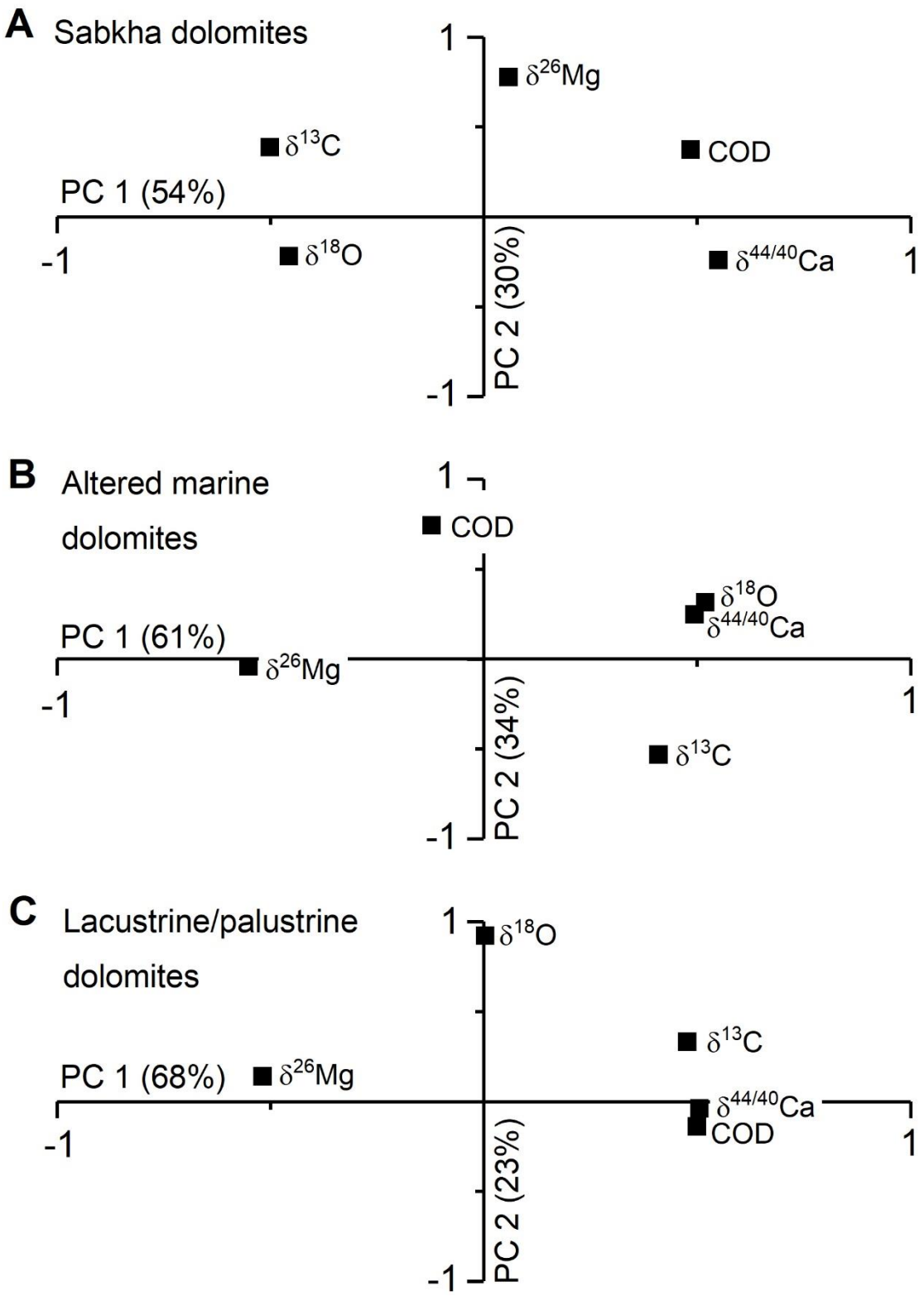

Figure 5: Principal Component Analysis (PCA) of cation ordering degree (COD), $\delta^{13}C$, $\delta^{18}O$, $\delta^{26}Mg$ and $\delta^{44/40}Ca$ of **(A)** sabkha dolomites, **(B)** altered marine dolomites, and **(C)** lacustrine/palustrine dolomites.

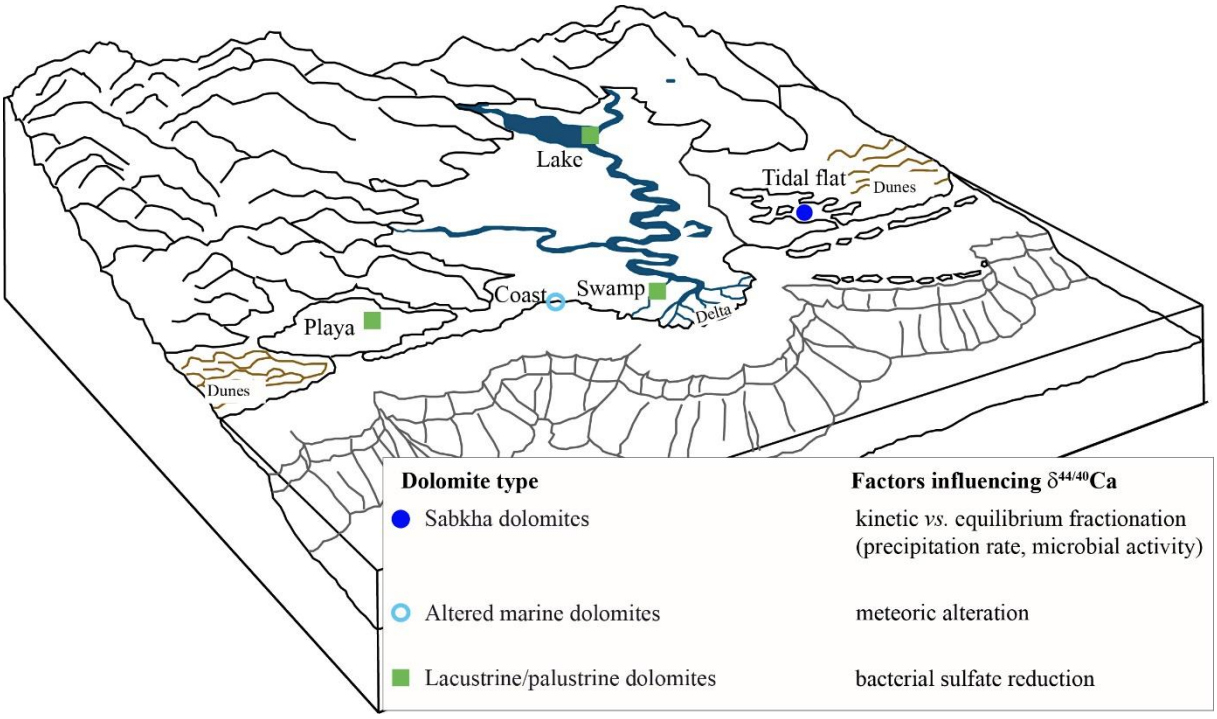

Figure 6: Schematic overview of the different dolomite types studied herein and their respective formation environment and main factors controlling the Ca isotopic distribution. Modified after Geske et al. (2015a).